Quaternary Science Reviews 105 (2014) 26–47

Contents lists available at ScienceDirect

Quaternary Science Reviews

journal homepage: www.elsevier.com/locate/quascirev

The latest LGM culmination of the Garda Glacier (Italian Alps) and the onset of glacial termination. Age of glacial collapse and vegetation chronosequence

Cesare Ravazzi [a, *], Roberta Pini [a], Federica Badino [a], Mattia De Amicis [b], Laurent Londeix [c], Paula J. Reimer [d]

[a] C.N.R. – Istituto per la Dinamica dei Processi Ambientali, Laboratory of Palynology and Palaeoecology, Piazza della Scienza 1, 20126 Milano, Italy
[b] DISAT, University of Milano Bicocca, Piazza della Scienza 1, 20126 Milano, Italy
[c] Département de Géologie et Océanographie, UMR CNRS 5805, Université Bordeaux 1, Avenue des Facultés, 33405 Talence cedex, France
[d] Centre for Climate, the Environment & Chronology School of Geography, Archaeology and Palaeoecology, Queen's University of Belfast, 42 Fitzwilliam Street, Belfast, UK

ARTICLE INFO

Article history:
Received 20 June 2014
Received in revised form
13 September 2014
Accepted 17 September 2014
Available online 7 October 2014

Keywords:
Alpine deglaciation
Vegetation history
Lateglacial
Reworked palynomorphs
Bison priscus
Heinrich Event 1

ABSTRACT

In the deglacial sequence of the largest end moraine system of the Italian Alps, we focused on the latest culmination of the Last Glacial Maximum, before a sudden downwasting of the piedmontane lobe occupying the modern lake basin. We obtained a robust chronology for this culmination and for the subsequent deglacial history by cross-radiocarbon dating of a proximal fluvioglacial plain and of a deglacial continuous lake sedimentation. We used reworked dinocysts to locate sources of glacial abrasion and to mark the input of glacial meltwater until depletion. The palynological record from postglacial lake sediments provided the first vegetation chronosequence directly reacting to the early Lateglacial withdrawal so far documented in the Alps.

Glacier collapse occurred soon after 17.46 ± 0.2 ka cal BP, which is, the Manerba advance culmination. Basin deglaciation of several overdeepened foreland piedmont lakes on southern and northern sides of the Alps appears to be synchronous at millennial scale and near-synchronous with large-scale glacial retreat at global scale. The pioneering succession shows a first afforestation step at a median modeled age of 64 years after deglaciation, while rapid tree growth lagged 7 centuries. Between 16.4 ± 0.16 and 15.5 ± 0.16 ka cal BP, a regressive phase interrupted forest growth marking a Lateglacial phase of continental-dry climate predating GI-1. This event, spanning the most advanced phases of North-Atlantic H1, is consistently radiocarbon-framed at three deglacial lake records so far investigated on the Italian side of the Alps. Relationships with the Gschnitz stadial from the Alpine record of Lateglacial advances are discussed.

1. Introduction

The major prealpine lakes of the Alpine forelands occupy glacially overdeepened basins (Preusser et al., 2010) framed by remarkable composite end-moraine systems, mostly built up during the Last Glacial Maximum (spanning from 30 to 18 ka cal BP, Lambeck et al., 2002; Schaefer et al., 2006; LGM onwards). The addition of morainic ridges to composite end-moraines and the subsequent withdrawal from major lake basins formed several sedimentary archives documenting the deglacial sequence. Continuous stratigraphic lake records preserved there reveal the ecological history of deglaciated terrains and provide proxies for climate events triggering the last glacial/interglacial transition (Schmidt et al., 2012; Ammann et al., 2013).

There is still considerable uncertainty about the timing of last glacial stadials testified in the end-moraines at about 18/21 ka cal BP before the onset of glacial termination (Ivy-Ochs et al., 2008). Phases of dramatic glacial collapses and paraglacial rearrangements marked the landscape of Alpine forelands and of valley floors at the termination onset. This phase of intensified deglaciation has been consistently patterned by re-investigation of stadial type localities (Reitner, 2007), but correlation of regional frameworks in the

* Corresponding author.
E-mail address: cesare.ravazzi@idpa.cnr.it (C. Ravazzi).

http://dx.doi.org/10.1016/j.quascirev.2014.09.014
0277-3791/

Alpine districts is not easy due to limitations and uncertainties in dating (Heiri et al., 2014 for an overview). This is apparent when the northern and southern Alpine realms are compared. An attempt to paleoecological N/S Alpine correlation down to 17 ka cal BP (Vescovi et al., 2007) highlighted a striking diversity of ecosystems and climate patterns during the Greenland Interstadial 1 and the Younger Dryas. Marked differences concern the persistence of forest throughout the LGM and Lateglacial in the SE-Alps and the rainfall gradients (Kerschner and Ivy-Ochs, 2007), also affecting the glacier responses to millennial scale events (Monegato et al., 2007). The north of the Alps was treeless until the onset of GI1 (Ammann et al., 2013), thus the pollen signals of earlier events may not be detected and they are even more difficult to date.

In this paper we address the environmental and sedimentary change between the end of LGM and the early Lateglacial in the Garda end-moraine, the largest classical glacial system on the southern slope of the Alps (Fig. 1). We focused on the potential of closed intermorainic lakes to frame timing steps of deglaciation and to record the ecological succession of the deglaciated terrain. We develop a strategy to record the course of the local deglaciation by using dinocysts reworked from marine bedrock and we attempt to radiocarbon date as closely as possible to deglaciation in order to reduce the deglacial lag, thus avoiding the problem of minimum age. To add consistency to the timing frame, we cross-correlate the onset of deglaciation in the proglacial lake and in the outwash plain, damming the lake itself.

We insist that pollen records from small and closed intermorainic lakes should record the vegetation pioneering at glacial withdrawal and the subsequent ecological succession, provided that sedimentation is continuous and that no change occurs in pollen sedimentation (i.e. floated pollen brought by lake inlets). We show that once the vegetation chronosequence is established, further evidence of independent perturbation may become apparent, testifying to climate events not yet stratigraphically documented in the Alpine early Lateglacial.

2. The Quaternary glaciation of the Garda basin

The Garda Lake (65 m a.s.l.), the largest lake of Italy, is hosted in a NE-SW basin cut through the sedimentary cover of Eastern Southern Alps, spanning from Triassic to Pliocene, and including minor volcanic bodies (Fig. 2a). It was deformed in form of an asymmetric syncline, trending NNE-SSW, and thus dissected by thrusts (Fig. 2b; Castellarin and Cantelli, 2000; Castellarin et al., 2005). This structure has driven the development of the main fluvial axes and valley glaciers. Beginning from the late Early Pleistocene, the Garda basin was reached several times by an Alpine glacier bearing increasing amounts of porphyries and granitoids from the volcanic platforms and the crystalline axial belt of the Alpine chain (Baroni and Cremaschi, 1987, see Fig. 1b). Multiple Middle and Late Pleistocene glacial advances spread at the southern Alpine border with a piedmontane lobe, the major on the southern Alpine side (Figs. 1 and 2a). The age of the morainic arcs of this typical composite end-moraine has been intensively debated (Penck and Brückner, 1909; Venzo, 1965; Habbe, 1969; Cremaschi, 1987; Accorsi et al., 1990; Bini and Zuccoli, 2004).

2.1. The last glaciation end-moraine system

The south and eastern margins of the end-moraine system culminate with a sharp ridge facing the outwash plain. The Solferino stage (Cremaschi, 1987) encompasses both this maximum glacier culmination and the subsequent inner arcs. A multiple geochronometric study (radiocarbon, OSL and IRSL dating) of the loess buried by till at Val Sorda (Accorsi et al., 1990; Ferraro, 2009, see position in Fig. 2a), established that the outer ridged belt of the

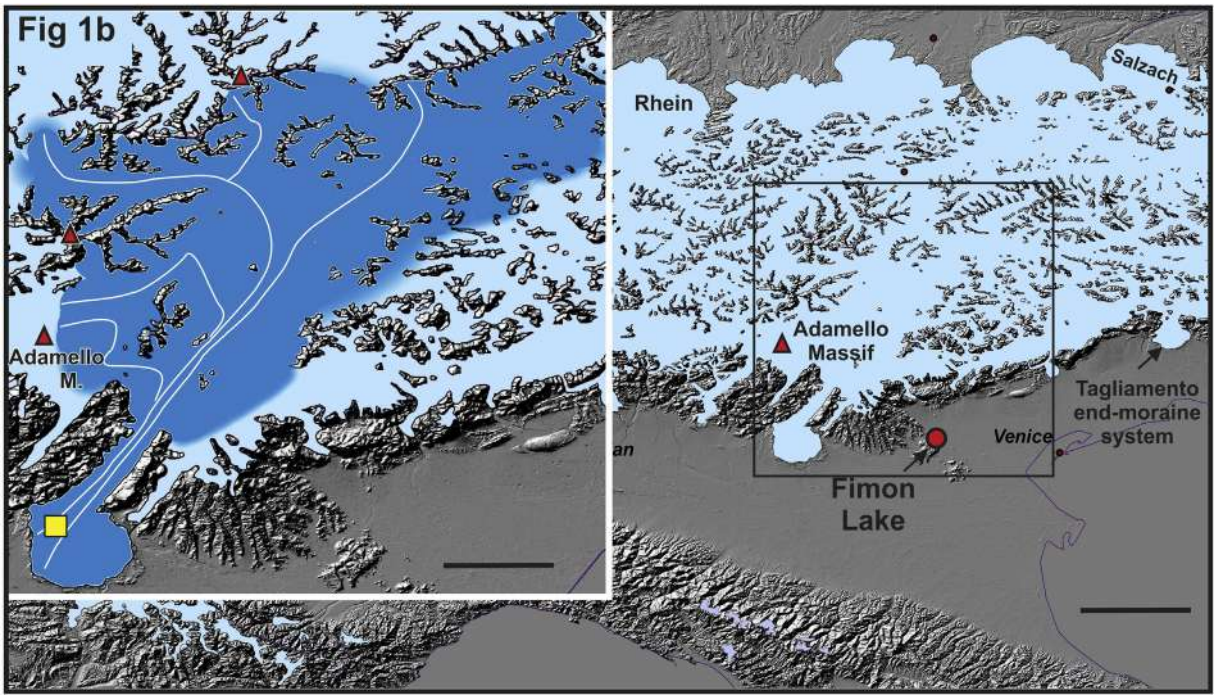

Fig. 1. Maximum extent of the last glaciation in the Alps (from Elhers and Gibbard, 2011) and detail of last glaciation catchment (Fig. 1b) and flow lines (based on Castiglioni, 1940). The pedemontane lobe of the Garda glacier is detailed in Fig. 2. The Manerba promontory is shown by a yellow square. (For interpretation of the references to color in this figure legend, the reader is referred to the web version of this article.)

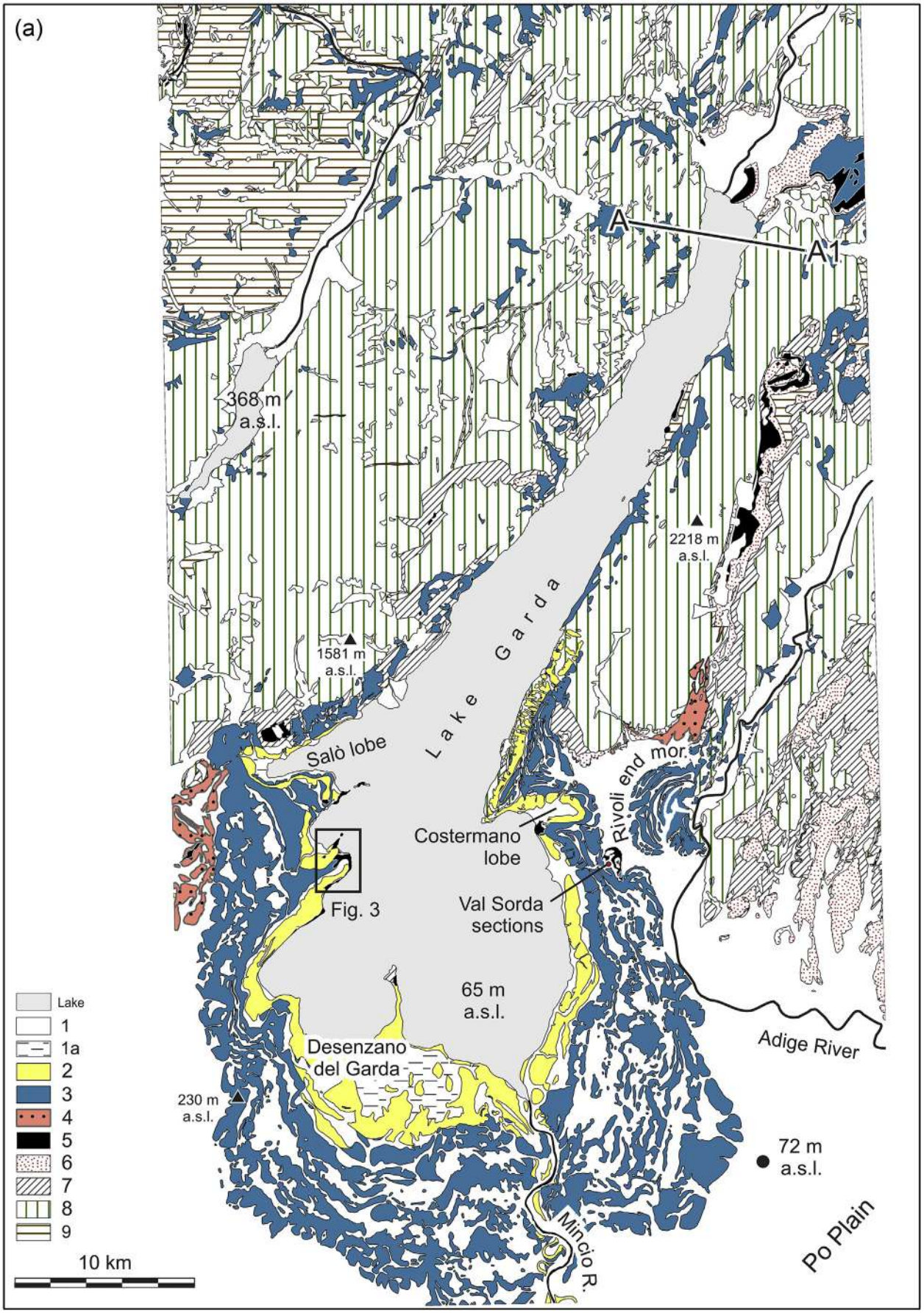
(a)
A
A1
368 m a.s.l.
2218 m a.s.l.
1581 m a.s.l.
Lake Garda
Salò lobe
Rivoli end mor.
Costermano lobe
Fig. 3
Val Sorda sections
65 m a.s.l.
Desenzano del Garda
230 m a.s.l.
Adige River
72 m a.s.l.
Mincio R.
Po Plain
Lake
1
1a
2
3
4
5
6
7
8
9
10 km

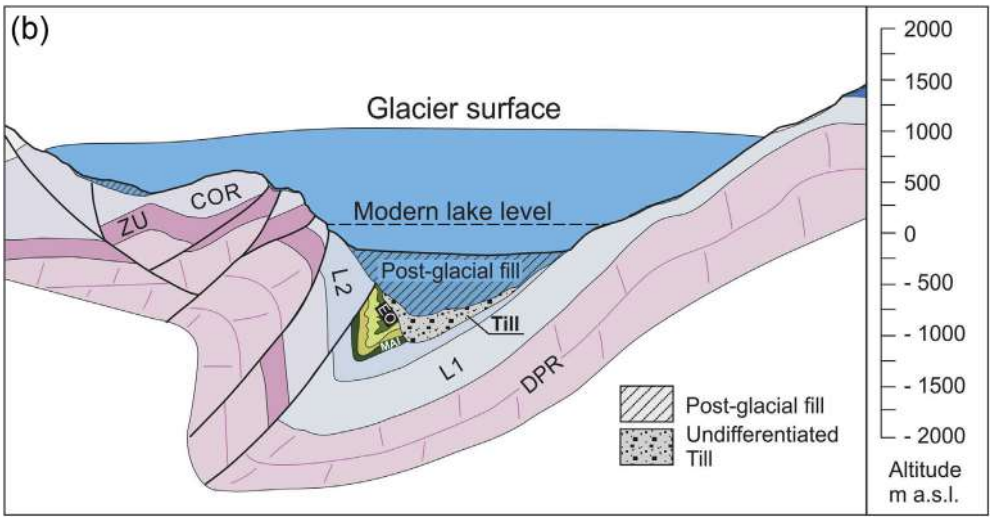

Fig. 2. (*continued*).

eastern end-moraine was formed after 32 ka cal BP, i.e. in the Last Glacial Maximum (LGM onwards).

Thanks to the continuity of the outer LGM morainic ridge, a correlation of paired elements of the end moraine on its W and E-lateral sides is feasible. Similar altitude gradients suggest a symmetric radial slope for the LGM piedmont glacial lobe (reconstructions in Habbe, 1969; see Fig. 14). Inside the main ridge, further morainic arcs alternate to outwash channels and hollows developing either ephemeral ice-contact lakes or permanent closed lakes isolated from the main hydrographic network. Coring closed basins down to meltwater detrital fine silts provided ages of 13.390 ± 70 yr ^{14}C BP (Baroni et al., 2006), and 13.280 ± 70 (Valsecchi et al., 2006, see Fig. 2a). Accordingly, the oldest palynological records pre-date the Bølling-Allerød interstadial complex (Bertoldi, 1968; Grüger, 1968; Valsecchi et al., 2006). However, the transition from ice contact drift to autochthonous lake sedimentation was neither investigated, nor directly dated.

Uniboom seismic profiles in the modern Lake Garda basin identified heterometric glacial deposits and their boundary to the overlying fine lacustrine succession (Curzi et al., 1992). In the SW and SE lake sectors, only small hills, with less than 10 m relief, were seismically detected beneath the postglacial lake sediments. This is insignificant compared to the relief of the morainic ridges surrounding the Lake Garda.

3. Methods

3.1. GIS survey, coring and lithostratigraphy

The topography of the end moraine system (scale 1:5000) and the available geological map for the Garda basin (Cadrobbi et al., 1948; Venzo, 1965; Servizio Geologico d'Italia, 1969; scale 1:100.000) were acquired in digital form. We generated a Digital Terrain Model and a Hill Shaded Model. Glaciated surfaces were computed into stratigraphic classes and relative areas were calculated either for the LGM maximum and for two subsequent stages mapped in Fig. 2a.

The studied intermorainic lake basin was drilled by technical rotation and by piston and russian corings, down to a depth of 10 m. We georeferenced 19 corings by a TOPCON GPT-300TN total station and acquired lithostratigraphic logs (sediment color, grain size, structures, macrofossils), which were correlated along W–E and N–S transects.

The lowermost segments of cores PAUL 14 and PAUL 19 were logged for image analysis, thermogravimetry, magnetic susceptibility and submitted to a detailed palynostratigraphic study. Susceptibility was measured with a Bartington MS2 susceptimeter equipped with a MS2E sensor operating on a 2 kHz frequency. Measures were taken every cm and repeated twice. High-resolution pictures were processed for gray-scale analysis with the software IMAGE J (Rasband, 1997–2014).

Thermogravimetric loss-on-ignition was determined with an automated LECO TGA 601 analyzer through subsequent steps of heating at 105 °C, 550 °C and 980 °C. TOC and carbonate contents were calculated stoichiometrically (Dean, 1974, 1999).

Nomenclature of lake sediments follows Kukal (1971) and Schnurrenberger et al. (2003). Stratigraphical concepts introduced in this paper conform to the event stratigraphy procedures (Walker et al., 1999).

3.2. Radiocarbon dating and age-depth model

The radiocarbon chronology of the studied core sections are based on four ^{14}C AMS dates obtained on terrestrial plant macrofossils, wood and charcoal (Table 1). The use of upland plant remains yielded accurate and precise ages, avoiding both reservoir or hard-water effects, and admixture of organic particles of various age, as for bulk samples. Macrofossils were rinsed with weak acid

Fig. 2. Simplified lithostratigraphic map of the Garda area. Key: 1 – Outwash, glacifluvial, alluvial plains and intermorainic lacustrine basins; 1a – Partly varved lacustrine deposits (last Lateglacial); 2 – Inner LGM glacial ridge (Manerba advance, end of LGM); 3 – Glacial ridges forming the composite end-moraine system (LGM); 4 – Glacial and ice-contact deposits (Middle Pleistocene); 5 – Marine limestones, calcarenites and continental conglomerates (Oligocene-Miocene); 6 – Marine calcarenites, clays and basaltic tuffs (Eocene); 7 – Clayay shales and limestones (Cretaceous); 8 – Limestones (Triassic-Giurassic); 9 – Volcanic-volcanoclastic rocks (Permian), sandstone-limestone (Early Triassic) and granodioritic batholite (Oligocene). Compiled after Cadrobbi et al., 1948; Servizio Geologico d'Italia, 1969; Cremaschi, 1987; Callegari et al., 2002; Castellarin et al., 2005 and the results of the present work. Fig. 2b – A-A1 section across the Garda sinclyne, showing the LGM trimline (structural pattern and trimline based on Habbe, 1969; Castellarin et al., 2005). Lithostratigraphic bedrock acronyms: DPR = Dolomia Principale; L1 = Lias 1; L2 = Lias 2; Zu = Calcare di Zu; COR = Corna; MAI = Maiolica; EO = Eocene.

while charcoal and wood samples were treated with a sequence of acid, base, acid. The samples were then rinsed in Milli-Q® water. All samples were dried, combusted to CO_2 in a sealed quartz tube with an excess of CuO, converted to graphite and then AMS-dated. Calibration was carried out with the program CALIB (v. 7.0.1, Queen's Univ. of Belfast), using the IntCal13 calibration data set (Reimer et al., 2013). We designed a Bayesian deposition model using the Oxcal 4.2 program (Bronk Ramsey, 2008). Although no hiatuses or major deposition changes could be detected, we adopted a Poisson sequence flexible model, with a low K parameter. This methodology also allowed calculating the modeled age of the main biochronological events found by the paleobotanical study (Table 2). The model could not account for century-scale changes in sedimentation rate which are apparent from the lithostratigraphic record (i.e. dark banding in the interval 595 to 548 cm depth PAUL 14) and from the correlated concentration peaks of pollen, charcoal and non-pollen palynomorphs. The analysis of these fine modulations will deserve further work.

We obtained a radiocarbon age from a *Bison priscus* skull collected during quarrying activities in a thick gravel sequence (see site position in Fig. 3b) whose deposition is related to the morainic dam at the culmination of the Manerba advance (see Section 5.1). A hard segment of dense bone was sawed from the articular surface to the right mandibular condyle (Fig. 4). After scraping the surface the bone was then subjected to a soxhlet solvent extract to remove contaminants as described in Bruhn et al. (2001). The bone was demineralized to eliminate the mineral components, treated with 0.1% NaOH to remove humic acids, gelatinized in weak HCl and ultrafiltered using a Vivaspin® filter. After freeze-drying the sample was converted to graphite as described above and analyzed by AMS.

3.3. Palynological analysis

3.3.1. Distinguishing reworked palynomorphs

The base of the studied core sections contains both well-preserved, primary-deposited pollen grains, and poorly-preserved reworked palynomorphs (mainly marine dinocysts). Characterizing these two components is essential for a straightforward evaluation of ice-contact debris supplied by glacially-abraded marine sediments, as well as to reconstruct the vegetation history at time of deglaciation. See Appendix B for criteria to distinguish reworked items.

3.3.2. The record of primary-deposited palynomorphs

The palynological record from core PAUL 14 is based on 72 samples analyzed for pollen, spores, algae, non-pollen palynomorphs, microcharcoal particles. Sediments were added with *Lycopodium* tablets for concentration estimates (Stockmarr, 1971), and treated according to standard methods, including HF and acetolysis. Pollen, stomata and algae were identified using reference European pollen floras and specialized keys (see Appendix B). Preservation of primary deposited palynomorphs is excellent.

Two size-classes of black and opaque charcoal particles (length between 10–50 μm and 50–250 μm) were counted in pollen slides; total charcoal concentration was calculated.

Pollen diagrams were drawn using Tilia 1.7.16 (Grimm, 1991–2011); percentages are based on a pollen sum including trees, shrubs and all upland herbs. Pollen sum (excluding aquatic and wetland species) reaches 600 ± 80 pollen grains. Pollen zonation was obtained by a constrained incremental sum of squares cluster analysis, using the Cavalli-Sforza's chord distance as dissimilarity coefficient (CONISS, Grimm, 1987). Clustering was restricted to taxa whose pollen reached over 2%.

3.3.3. Analysis of dinoflagellate cysts

Dinoflagellate cysts (dinocysts) were used as a tracer of marine bedrock abrasion and thus of meltwater supply as well. The stratigraphical occurrence of each dinocyst taxon has been statistically estimated on the base of its occurrence-index, i.e. a frequency ratio between occurrences and the total number of geological sequences available in a reference database. That database includes 9822 dinocyst records from 287 worldwide geological sections selected for their accurate (and non dinocystal) biozonation (e.g. Alberti, 1961; De Coninck, 1975; Manum et al., 1989; Van Simaeys et al., 2005). More than 1555 taxa are considered whose total occurrence spans a Carnian to Holocene stratigraphical range. In order to identify source rocks contributing to the reworked associations, the sample dinoflagellate fossil flora was compared with the respective occurrence-index of each taxon. This innovative approach offers the advantage of obtaining a relatively precise dating (stage level) with a small number of species, and it is a way of getting round the presence of stratigraphical index species.

4. Results

4.1. The lake-edging morainic ridge and related dammed ice-contact lakes

A sharp morainic arc, culminating at 130–115 m a.s.l., edges 50–70 m over the western and eastern shore of the modern Garda Lake (65 m a.s.l.). The related glacial and outwash bodies could be correlated throughout the end-moraine system under the event name of Manerba advance (number 3 in Fig. 2a). Topographically, our survey is consistent with an earlier map (Venzo, 1957, 1965). Steep slopes, aligned to NE-SW trending fault belts (Curzi et al., 1992), edge the western Garda Lake shore and mark lateral accumulation to the SW-directed glacial flow. Instead, terminal positions (Desenzano del Garda) and lateral inlets (i.e. the gulfs of Salò and Costermano, Fig. 2a) show gentle slopes and preserve glacial varves (Venzo, 1965, see number 1a in Fig. 2a), cropping out at altitudes of about 10 m above the current lake level. Suspended fan deltas and relict notches dating from early Lateglacial to middle Holocene are known in a belt of 50 m above the modern lake level, thus implying a substantial lake level fall from the Lateglacial onwards (Baroni, 2010; see Fig. 3b). Consistently, outwash deposits occur only outside the Manerba ridge at 115–130 m a.s.l. They are formed by crudely stratified, poorly sorted gravels. A 10 m thick exposure of an outwash sequence, quarried in the 1950's (see position in Fig. 3b), yielded a bison skull (*Bison priscus*, Fig. 4) which allowed a radiocarbon age for the culmination of the Manerba advance (Table 1).

Outwash plains support a cover of alfisols (Hapludalf), or degraded entisols (Udarent) originated by plowing. Unplowed gentle morainic slopes preserve B_t and BC_t illuvial horizons up to 0.8 m thick, formed by 5 YR-clay and hydroxides (ERSAL, 1997); their colluvial wedges, up to 2 m thick, rest at slope base, over fully developed calcic C_k horizons or polished calcarenite bedrock (Sasso di Manerba, see Appendix A). The prevailing soil processes are moderate leaching, accumulation of residual hydroxide, hematite formation, and precipitation of friable carbonate at the profile base, reaching level III according to Gile et al. (1966). These pedogenetic properties are related to limestone parent material and to a seasonally contrasted, temperate climate prevailing in the last postglacial (Cremaschi, 1987; ERSAL, 1997). On the other hand, our data drop earlier statements restricting rubefied alfisols to older (i.e. pre-LGM) terrains (Venzo, 1965; Mancini, 1969).

Table 1
Ages obtained by ^{14}C AMS-dating of plant macrofossils from the PAUL 14 core and of collagene from a *Bison* skull, along with 2-sigma calibration ranges and median probability ages.

Lab code	Sample position and depth	Dated material	Dry weight (g)	^{14}C ages (uncal years BP)	Calibration range (2 sigma, cal years BP, relative area %)	Median probability (cal years BP)
UBA 17905	PAUL 14,485 cm	wood	0.109	12,115 ± 50	13,793–14,128 (100%)	13,982
UBA 20790	PAUL 14,534 cm	wood and charcoal	0,0981	13,136 ± 63	15,515–16,025 (100%)	15,776
UBA 17904	PAUL 14,566 cm	charcoal	0.058	13,994 ± 69	16,665–17,250 (100%)	16,993
UBA 20791	PAUL 14,591–592 cm	*Hippophaë* seed and leaf fragment	0,0085	14,351 ± 72	17,216–17,712 (100%)	17,489
UBA 25356	Crociale 8 m	Condyle of *Bison* skull	2,8408 (4% collagene content)	14,288 ± 109	17,064–17,707 (100%)	17,398
	(end Manerba stage culmination)	Mean pooled UBA 20791 and UBA 25356		14,331 ± 60	17,226–17,656 (100%)	17,465

Several lake basins were formed at the culmination of the Manerba advance, or just after the subsequent retreat, three of them stratigraphically investigated so far (Figs. 2a), i.e. Lake Frassino (Baroni et al., 2006), Lake Lavagnone (Arpenti et al., 2004), and Lake Paùl di Manerba (this work).

4.2. Lithostratigraphic assessment of the Paùl di Manerba basin fill

The moraine belonging to the Manerba advance is lapping on the Oligocene limestone bedrock forming the Rocca di Manerba hill (Fig. 3). A bedrock platform scoured by glaciation, sculptured by whalebacks on exposed highs, is cut by a coastal cliff, 40–55 m high, plunging in the Garda Lake. The Paùl di Manerba basin is framed down-the-glacier flow by the Manerba advance moraine and upward by the bedrock platform (Fig. 3b). The basin bottom is coated by lodgement till, as shown by drilling PAUL 14 (Figs. 3, 5 and 6). At the time a karstic outlet drained the lake through a dolina. However, most probably the dolina remained sealed by glacial sediments a long time after deglaciation. The lake was filled by limnic carbonates until reclamation in the XVII century.

Two perpendicular drilling transects across the lake filling (Fig. 5) found a limnic succession almost entirely formed by chemical and biochemical precipitated carbonate mud with fine organic matter (Lithozone L3 in Fig. 6). The detrital component was roughly estimated by the LOI silicoclastic residue and by magnetic susceptibility in two selected cores close to the ancient littoral belt (PAUL 14 and 19). Here, micas and magnetite abraded from the crystalline and volcanic rocks mark meltwater silts with susceptibility peaks over 20×10^{-5} unit SI, together with a siliciclastic residue about 70% of dry sediment (Lithozone L2 in Fig. 6). The sharp contact L2/L3 between siliciclastic silt and carbonate mud represents the final event of meltwater supply depletion in both cores. Moderate peaks of siliciclastic residue and susceptibility in the first meter above the contact (M1 to M4 within Lithozone L2 in Fig. 6) suggest recycling of detrital sediment, as also shown by co-occurrence of reworked marine microfossils (see section 5.4). A characteristic color-banding is apparent in the lower Lithozone 3 (L3a), but absent in the uppermost 5 m of homogeneous light carbonate mud (L3b). Darker bands do correlate to higher organic matter content and possibly to decreasing redox potential as well. In shallow lakes, bands of organic-sulphidic mud and light carbonate muds mark phase alternance of poorly oxygenic and oxyc-distrophic lake bottom (Hakanson and Jansson, 1983). Sediment banding allowed fine correlation between PAUL 14 and 19 cores (Fig. 6). The reconstructed geometry implies Lateglacial deposition of a carbonatic prisme on the littoral lake shore. The development of a littoral carbonate platform is commonly observed in carbonate-saturated, shallow belts of temperate lakes (Dean and Fouch, 1983; Talbot and Allen, 1996). Furthermore, by correlating the L2/L3 transition in the studied cores, we could exclude hiatuses or erosion at the limit surface between detrital meltwater silt and the overlying autochthonous precipitated carbonate succession.

Table 2
Vegetation chronosequence modeled chronology. μ = arithmetic media; σ = standard deviation; m = median. yrs a.d. = years after deglaciation.

Depth (cm)	Event modeled (or radiocarbon sample)	Calibrated range (95.4%)		μ	σ	m	Modeled range (95.4%)		Modeled statistics and time elapsed after deglaciation (yrs a.d.)			
		From	To				From	To	μ	σ	m	m (yrs a.d.)
485	UBA 17905	14,130	13,793	13,972	89	13,981	14,142	13,807	13,985	88	13,995	3560
494	Thermophilous broad-leaved trees expansion						14,634	14,010	14,312	156	14,303	3262
496							14,721	14,065	14,385	165	14,376	3179
524	Tree-*Betula* expansion						15,729	15,055	15,404	169	15,415	2140
526	End Ragogna oscillation						15,785	15,145	15,476	161	15,486	2069
534	UBA 20790	16,026	15,517	15,772	125	15,776	15,996	15,553	15,768	109	15,770	1785
537							16,140	15,615	15,872	129	15,870	1685
552	Onset Ragogna oscillation						16,715	16,074	16,394	161	16,396	1159
557	End *Larix* continuous						16,874	16,256	16,568	155	16,572	993
558							16,904	16,295	16,603	153	16,607	948
560							16,961	16,378	16,672	148	16,677	878
566	UBA 17904	17,255	16,655	16,984	141	16,993	17,101	16,638	16,881	119	16,885	670
574	End pine expansion						17,340	16,823	17,084	129	17,087	468
578	Onset pine expansion						17,442	16,921	17,186	130	17,188	367
590	Onset PA3						17,733	17,251	17,491	115	17,491	64
592	UBA 20791	17,715	17,216	17,484	120	17,490	17,782	17,318	17,542	109	17,520	35
596	Meltwater depletion						18,003	17,391	17,679	151	17,555	0

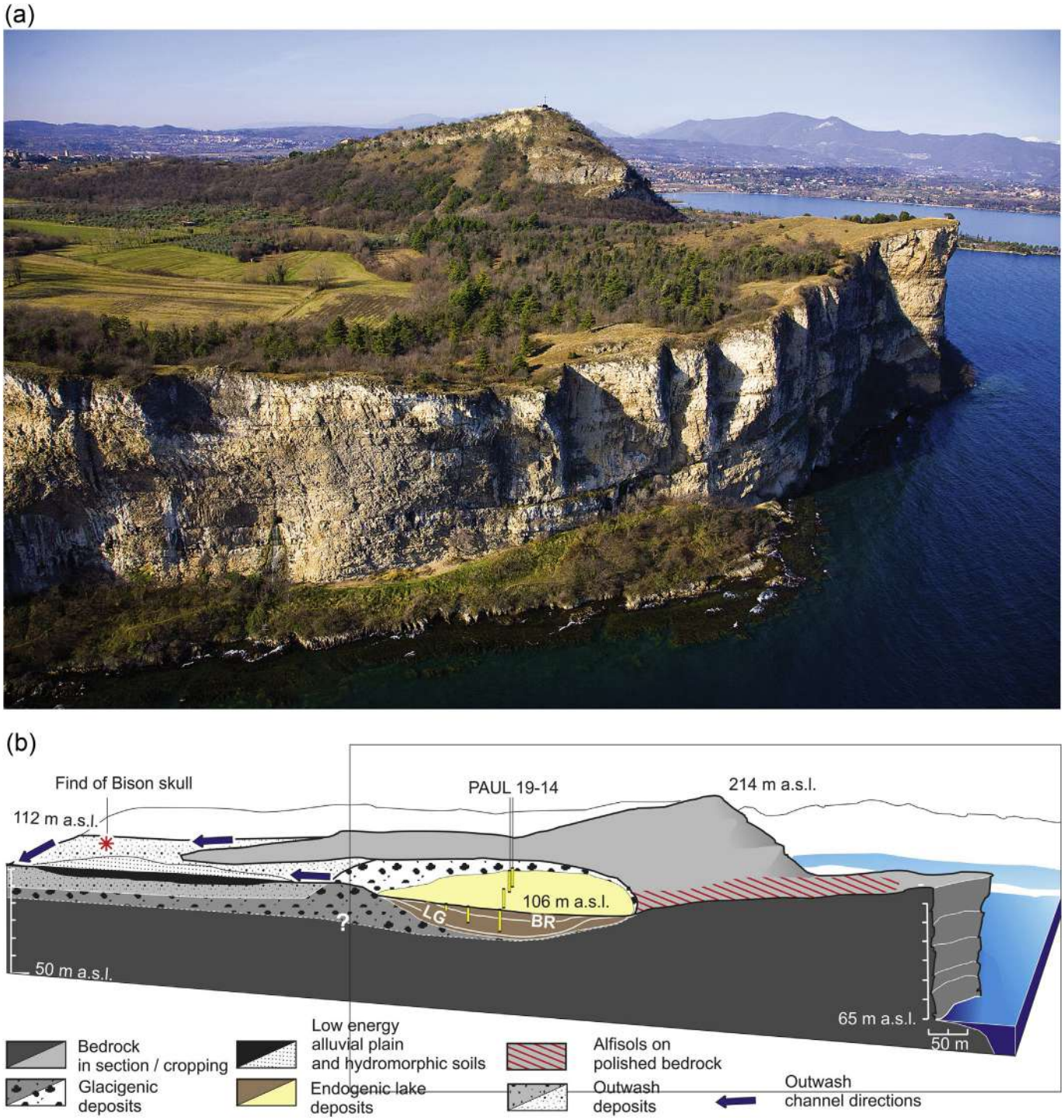

Fig. 3. (a) The Manerba promontory hanging over the Garda Lake viewed from the East (photocredit: Lino Olmo); On the left the lake basin Paùl, resting over the limestone pavement. (b) – Section showing the main geological bodies and landforms discussed in the text. Cliff arrows indicate the relict nocthes identified and dated by Baroni (2010). The Paùl Lake, in the center of the section, is filled by endogenic deposits. LG = Lateglacial; BR = Bronze Age.

4.3. Radiocarbon ages of the Manerba advance culmination and age-depth model for the deglacial chronosequence

Four radiocarbon ages were obtained from terrestrial plant items inbedded in lithozone L3a, i.e. the time spanning from meltwater supply depletion to Lateglacial interstadial GI-1 onset. Helpfully, the occurrence of woody plants in the glacier forefields of SE-Alps during the last glaciation (i.e. Monegato et al., 2007) provides the chance to find terrestrial plant debris mainly in littoral deposits, receiving debris from the nearby slopes. Of special importance is the find of a complete seed of sea-bucktorn (*Hippophaë* sp., Fig. 7) just 6 cm above the basal contact between meltwater silt and biochemic carbonates. Its age is indistinguishable from the one obtained from the *Bison* skull from the nearby outwash deposits.

Fig. 4. The skull of *Bison priscus* from outwash deposits at Manerba, anterior view (see Figs. 3b and 13a for site location). An arrow shows the articular surface to the right mandibular condyle, withdrawn for dating.

The age/depth model designed for the lake deposition since deglaciation (Fig. 8) shows envelop distributions of 220–370 yr and 300–450 yr for 68% and 95% probability ranges respectively (σ = 88–178 yrs). It provides a modeled chronology for the vegetation chronosequence since deglaciation (Table 2). The sample resolution of the pollen record is 50–70 yrs.

4.4. The record of Cenozoic dinocysts and of other reworked microfossils

Reworked palynomorphs – i.e. marine dinocysts, benthic foraminiferal linings, spores, pollen - are locally abundant in lithozone L1 (lodgement till) and abundant in L2 (detrital silt), while they are sporadic in L3a and limited to the interval from 558 to 510 cm depth in PAUL 14 (Fig. 6). Although only a few dinocysts were complete and well preserved, each sample yielded determinable remains at least to genus level. 68 dinocyst taxa were identified in total. Their overall stratigraphic range spans from lower Cretaceous to Quaternary. *Spiniferites* and *Homotryblium* are the most frequent genera, the latter mostly represented by *H. plectilum* and *H. tenuispinosum*, having their highest occurrence index in the Rupelian-Aquitanian. *H. aculeatum* and *Enneadocysta pectiniformis*, also common in most samples, have an optimal occurrence index in Priabonian-Rupelian. A plot of the dinocysts record according to their probable age (Fig. 9) suggests that most of the meltwater silt L2 reworked compound derives from rocks spanning from late Eocene to early Miocene (Fig. 9). Cretaceous, early Eocene and Pliocene rocks also provided a continuous contribution in L2 and L3a, but with a smaller amount of dinocysts.

4.5. Vegetation chronosequence on deglaciated terrain

The record of terrestrial/aquatic vegetation since deglaciation (Figs. 10 and 11) highlights the main stages of a chronosequence developed over the deglaciated terrain. Its modeled chronology (Table 2) allows estimating changes in airborne pollen rain with a time elapsed after deglaciation (Table 3). In Table 3 we also highlighted ecological constrains and events inferred from the overall match of lithostratigraphic and paleoecological evidence so far collected from core PAUL 14. In the foregoing chronology reference, we use the median of time elapsed after deglaciation (tm); see Table 2 for uncertainties.

The entire lake succession overlying the basal till is pollniferous; however, most of primary-deposited pollen in the meltwater silt (basal pollen zone PZPA1) was likely contained in ice and underwent floating, as shown by coeval abundance of reworked items; hence relative pollen abundance and changes do reflect taphonomical issues instead of vegetation histories (see light fill in pollen curves of Fig. 10). Most probably, enhanced flotation of saccate pollen (e.g. Ammann, 1994) affects the relative abundance of pine pollen compared to *Artemisia* in PZPA1.

Since PZPA1/PZPA2 limit (596 cm depth), pollen spectra represent prevailing airborne deposition in open littoral water. The inferred vegetation is formed by pioneer petrophytic herbs, steppe and by a *Hippophaë-Juniperus* scrub (see Table 2). Spread of *Pediastrum integrum* and *Botryococcus* in the aquatic realm reflects algae pioneering clean and cold water (Komárek and Jankovska, 2001) and promoted carbonate precipitation (Kelts and Hsü, 1978, Fig. 6). The PZPA1/PZPA2 limit will be given time = 0 yr in the vegetation chronosequence of the newly deglaciated terrain, although the tophill of the Rocca di Manerba likely hosted petrophytic vegetation since earlier LGM retreat phases. Pollen accumulation rates and % increases of *Artemisia* and *Juniperus* in PZPA2 reflect local colonization, while stable pine pollen % may result from background input, i.e. long-distance transport. First *Pinus sylvestris/mugo* stomata, testifying to pioneer individuals close to the site (Ammann et al., 2014), are recorded at the onset of PZPA3, median age 17.490 yr cal BP, i.e. at tm = 64 yrs.

Between tm = 367 and 468 yrs (late PZPA3, 574–578 cm depth), a sudden increase of AP from 35 to 65% marks forest growth (*Pinus* and tree *Betula*, with *Larix*), coupled to a contraction of steppe and scrub groove plants such as *Juniperus, Artemisia,* Gramineae, *Plantago alpina* type. However open habitats did maintain a significant input to pollen rain. A next step of AP increase and *Larix* expansion at tm = 660/878 yrs (PZPA4a, 566–560 cm depth) represents a further step of long-term forest thickening. Peaks in charcoal particles, anticorrelated to AP accumulation rate, indicate fire events affecting tree pollen production and biomass. These fires, however, do not interrupt the long-term trend of increasing forest density. This interval is matched in the sedimentation by darker bands, representing phases of gyttja accumulation in an anoxyc and productive hypolimnion.

Between tm = 1160 and 2070 yrs (PZPA4b, 552-526 cm depth, 16.396 to 15.486 cal yrs BP) a withdrawal of *Pinus cembra* is mirrored by a new moderate expansion of *Juniperus, Artemisia* and other xerophytes. This points to a recessional stage of millennial duration. In the aquatic belt, a slow increase of *Sparganium emersum*-type pollen points to expanding Alpine bur-reed species (e.g. *S. angustifolium*). The pollen representation of this species is low and insignificant in offshore cores (e.g. Nováková et al., 2013), but changes >0.5% are statistically significant in pollen counts >600 grains, as it commonly occurs in littoral oligotrophic successions. This rhyzophytic hydrophyte forms marshes on littoral platforms and its spread occurs during low-stand water level phases in oligotrophic lakes (Toivonen and Huttunen, 1995).

A subsequent expansion of tree-*Betula* marks the development of a mixed forest around the lake (PZPA5, since 15.490 cal yrs BP, tm = 2140 yrs).

About 12 centuries later, broad-leaved warm-temperate trees (*Quercus* and *Tilia*) start expanding (PZPA6, 14.300 cal yrs cal BP). In the southeastern Alps, their immigration was driven by the warming at the onset of Greenland Interstadial 1 complex (Vescovi et al., 2007).

5. Discussion

5.1. Dinocyst sources and accumulation as a marker of glacial activity and of meltwater mixing

The dinocysts record from till L1 and blue silt L2 allowed identifying the rock sources contributing to microfossil reworking. Now,

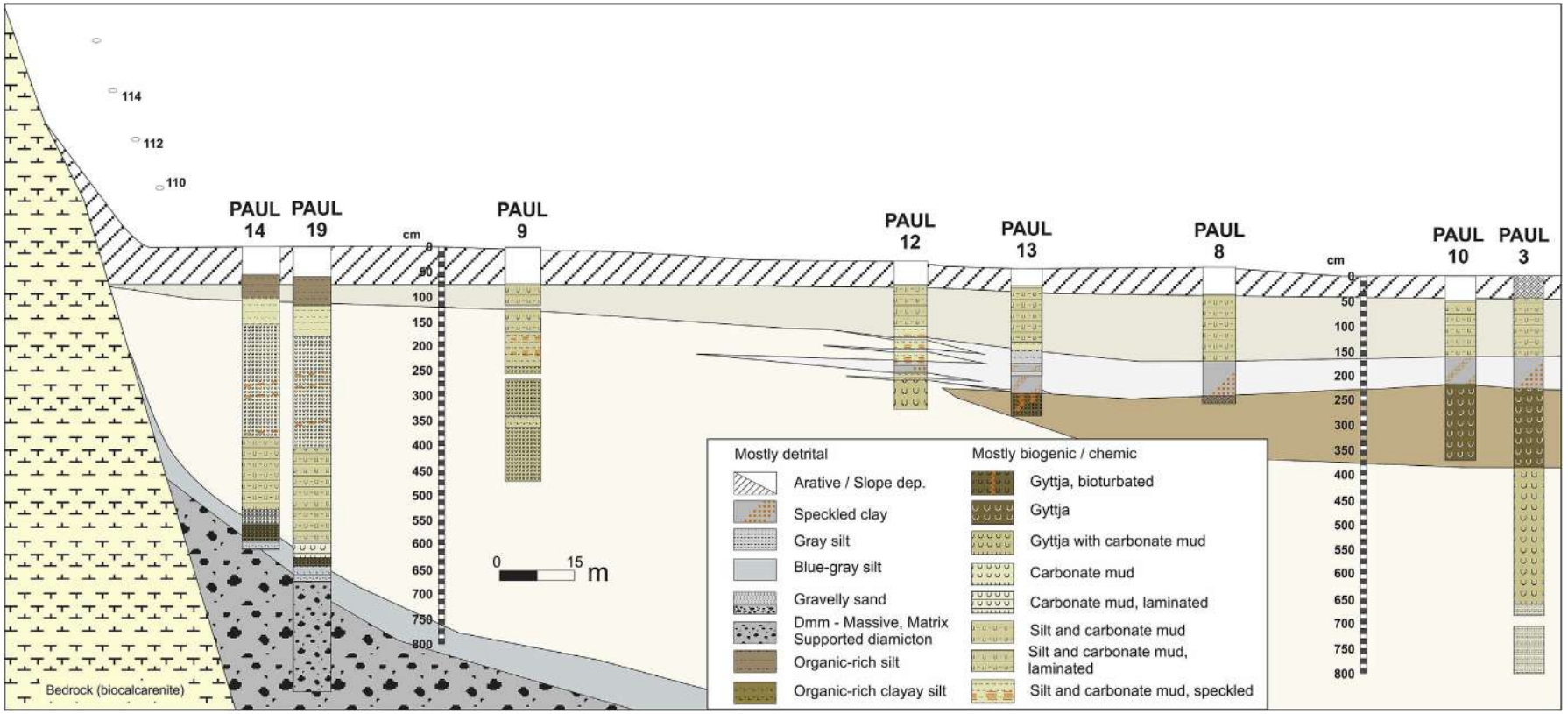

Fig. 5. W–E transect and litostratigraphic setting in the western Paùl basin.

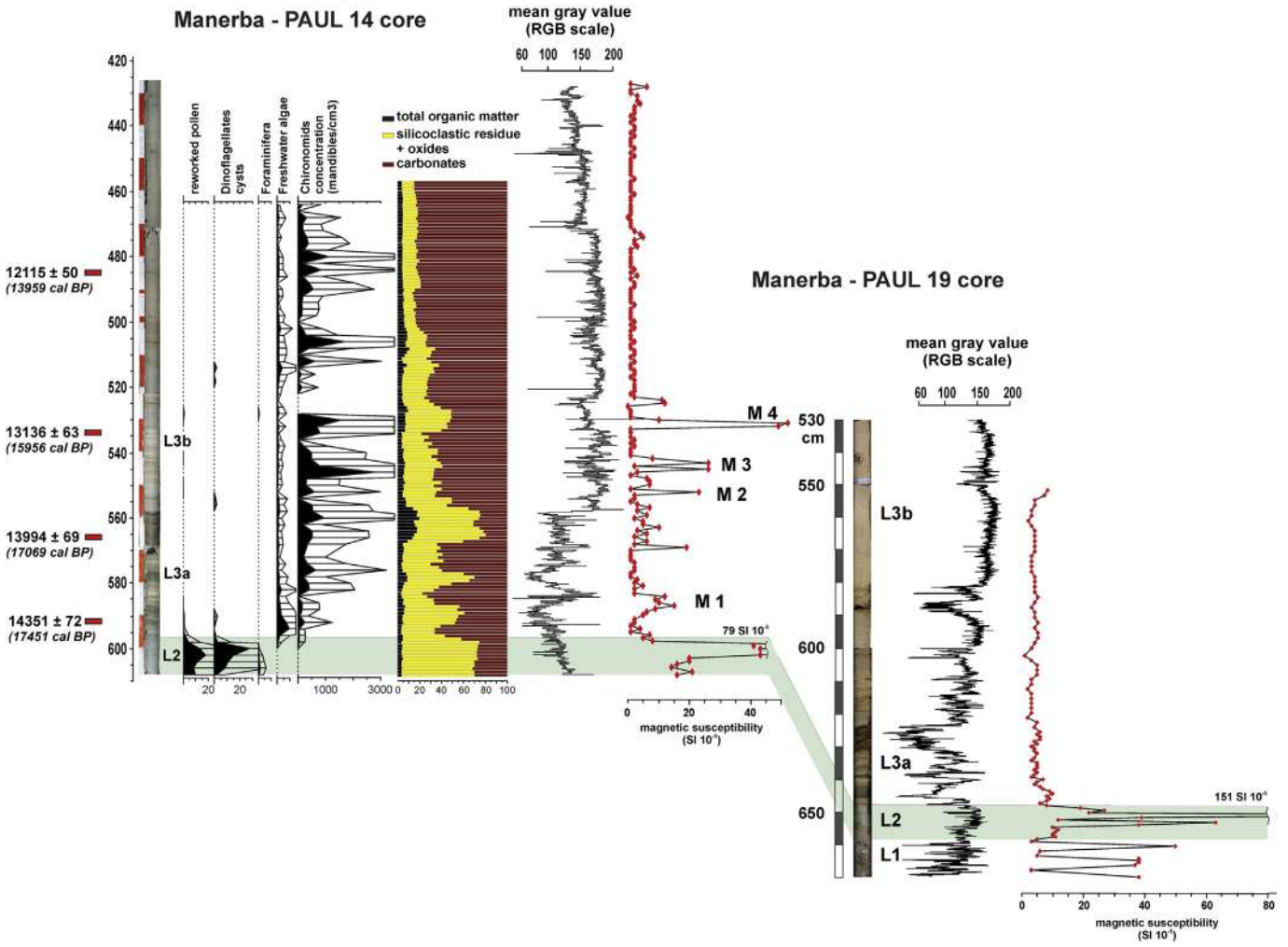

Fig. 6. Core logs PAUL 14 and PAUL 19 including lithostratigraphic proxies, position of dated samples, ages, and cumulative abundance of reworked microfossils. Total organic matter, carbonate and residue % contents refer to the dry sediment weight.

Fig. 7. The dated *Hippophaë* seed, 6 cm above the basal contact from meltwater silt to lake marl.

the question is upon whether their abundance and provenance may reflect glacial abrasion in time and space.

Given the chronostratigraphic sequence characterizing the area (Fig. 2), we compared the relative abundance of dinocyst age with the subsurface extent of marine rocks along the glacier flux of the Garda Lake basin (Fig. 12):

(i) A predominance of Oligo-Miocene dinocysts (Rupelian to Aquitanian) matches a rock source located within the axial syncline hosting the glacier tongue (see section in Fig. 2b). Moreover, these rocks form the basement of the Manerba promontory and of the lake basin up-to-glacier flow (dotted in Fig. 12);

(ii) Two different Eocene sources (Ypresian and Priabonian) and an Upper Cretaceous source are significant both in L2 dinocysts ages and in the rock sources, but not in lithofacies L1 (lodgement till);

(iii) Late Triassic and Jurassic dinocysts are absent, despite the abundance of rock sources over the entire glacial catchment area (Figs. 1b and 12). This may reflect both source distance along glacier flux and low primary concentration;

(iv) Almost constant finds of reworked Pliocene dinocysts in the glacial meltwater (lithofacies L2) provide evidence that a marine gulf was feeding the Garda basin at that time. As these items occur only in the meltwater silt and not in the till,

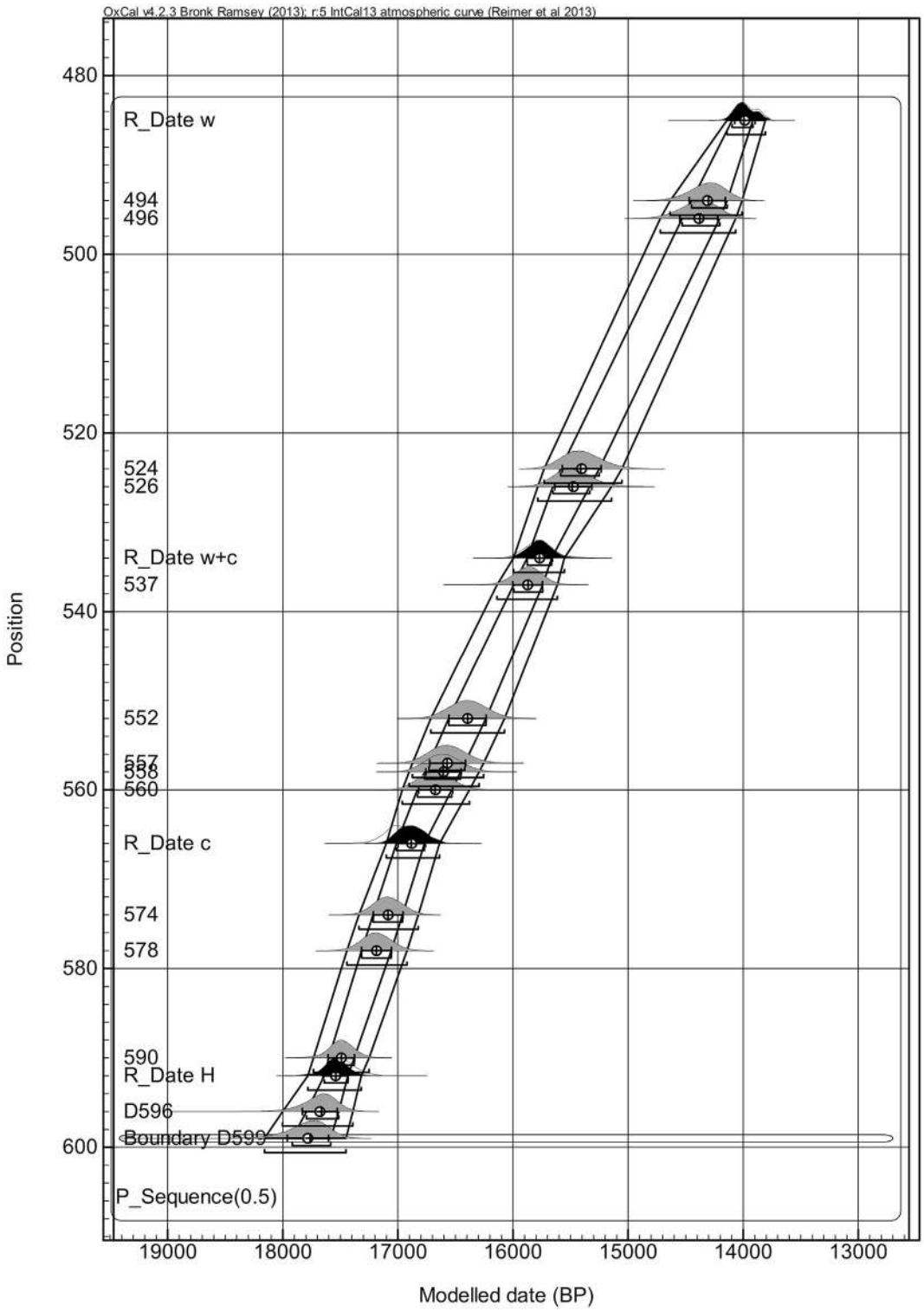

Fig. 8. Age-depth model based on radiocarbon ages (probability distributions in black) and modeled age of main biochronological events (probability distributions in gray).

it is argued that the relevant source was not up-to-glacier flow, but instead on a marginal area. This figure is corroborated by the occurrence of Pliocene marine deposits in the tectonically uplifted, unglaciated area facing west the Garda Lake (Baroni and Vercesi, 1995; Servizio Geologico d'Italia, 1969; see Fig. 2a).

From these data, it is concluded that the most relevant contribution of fine particles to blue silt L2 was provided through glacial meltwater by rocks overridden by glacier shortly upstream along the axial glacier flux. However, while L2 composition derives from a mixing of different meltwater sources, resulting in a multimodal distribution, the dominant till composition is

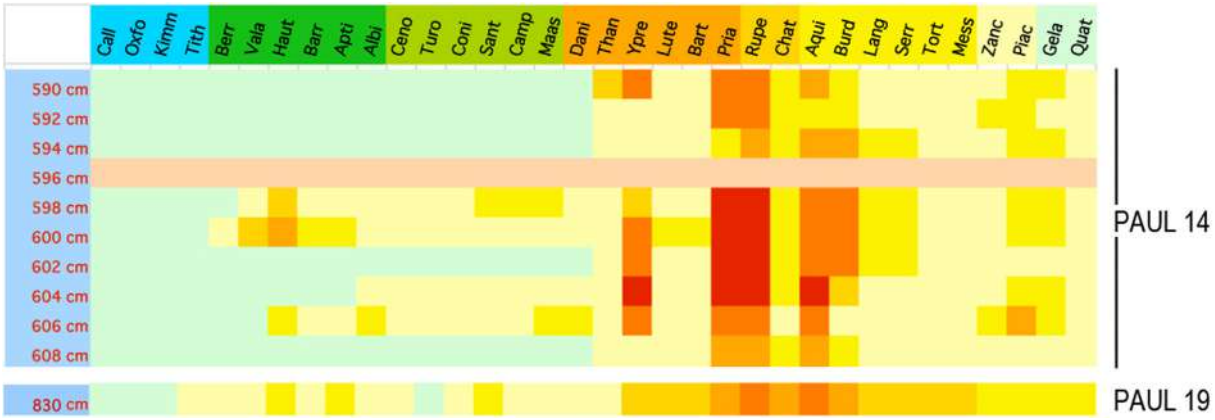

Fig. 9. Plot of the dinocysts record according to their probable age. Colors and gray tones show the most probable age of rocks delivering reworked dinocysts.

restricted to those microfossils directly delivered by subglacial erosion up-to-glacier flow. Here, source (i) is prevailing. Other potential sedimentary rock sources located in the glacial catchment area could be traced by dinocysts in blue silt (ii-iv). Their abundance in meltwater deposition reflects either primary microfossils concentration or subsurface extent of rock sources, and, again, the proximity of overridden rock sources along the glacial flux.

As far as fine silt production and reworked microfossils delivery are concerned, the lithogenetic properties of carbonate rocks are relevant. Subglacial friction over well-bedded and karstified carbonate bedrock and subglacial wash-out may allow for significant subglacial abrasion and delivery of fines. Basal sliding over carbonate rocks is implemented by low hardness and by active chemical processes enhancing either chemical and mechanical erosion (Hallet, 1976; Boulton, 1979; Eyles and Menzies, 1983; Sharp et al., 1995; Bennett and Glasser, 1996).

5.2. Deglacial lags in small lakes and related outwash – a short reappraisal

Deglacial chronologies using basal ^{14}C dates from lake cores are hampered by the minimum-age problem and by the hard-water effect on bulk organic matter (e.g. Fisher et al., 2009). Here, we address the advantages of using identifiable terrestrial plant debris in cores from intermorainic lakes hosted by end moraine systems.

Extracting terrestrial, identifiable plant debris from deglacial sequences is feasible in those regions that supported a woody cover throughout the LGM span (i.e. 30 to 18 ka cal BP) This is the case of southern and southeastern Alpine fringe (Sercelj, 1996; Monegato et al., 2007; Ravazzi et al., 2012; Monegato et al., in prep.). Radiocarbon AMS ages offer a precision hardly available today by other methods in the Alpine LGM and Lateglacial (see Kaiser et al., 2012). Still, getting a significant age for the deglaciation is a challenging task, even in a virtually continuous sediment record. Due to large changes in sedimentation rates, estimating the lag between deglaciation and the first macrofossil find may be unreliable, hence modern vegetation-soil chronosequences (e.g. Matthews, 1992; Moreau et al., 2008; D'Amico et al., 2014) are sometime used. However, this method provides only a minimum age for the deglaciation and is biased by comparing chronosequences developed under different climates.

To estimate the deglaciation lag, we took advantage of the following circumstances:

(a) A sudden decline of meltwater fine sediment supply in a closed intermorainic lake marks the boundary when glacier spillouts dried out, thus representing a non-lagged time marker for local withdrawal of the glacier front. Differently, large lakes formed in valley glaciers or overdeepenings were supplied by meltwater silt until complete deglaciation of the basin catchment. They do not provide markers for *in situ* deglaciation, but instead quantitative deglacial chronostratigraphies (in the Alps, Lister, 1988; Niessen and Kelts, 1989).
(b) Correlation of paired corings across the transition from detrital to authochtonous sedimentation allows checking for erosional events and/or onlap-type unconformities and estimating sedimentation rates until the first macrofossil find;
(c) A continuous record across deglacial transition in a vegetated area is expected to yield pollen evidence for primary succession of deglaciated terrain;
(d) A sequence of radiocarbon ages into deglacial authochtonous deposits allows designing a Bayesian depositional model to estimate the deglaciation lag and its time probability distribution.

Hopefully, plant or faunal remains may be preserved in outwash deposits strictly associated to deglacial lakes formation. *In situ* tree stumps may allow building glacial chronologies, as in the case of Holocene heavily vegetated landscapes (e.g. Wiles and Calkin, 1994; Holzhauser, 2010), but LGM proglacial environments were mostly treeless in the Alps. Further problems arise with time-correlation over distal outwash deposits and with reworking. Usually organic remains delivered to outwash deposits – as stem parts and shoots, conifer cones and bones - which were streamborne mark the age of the aggradation event, but clasts of older peat and wood fragments may also be easily reworked in glacial and fluvioglacial landsystems. These latter items are still useful to reconstruct well-constrained glacier histories (e.g. Hormes et al., 2001), but are unsuitable for deglaciation chronologies. Overall, the chance of dating an *in situ* tree stump or bone remains in a proximal outwash deposit offers the advantage to minimize the risk of both glacial reworking and reservoir effects.

For all these reasons, we believe that the congruent dates obtained for (1) the sudden decline of meltwater fine sediment supply in a closed intermorainic lake and (2) a skull from the associated outwash deposits provide a robust base for dating the Manerba glacial advance.

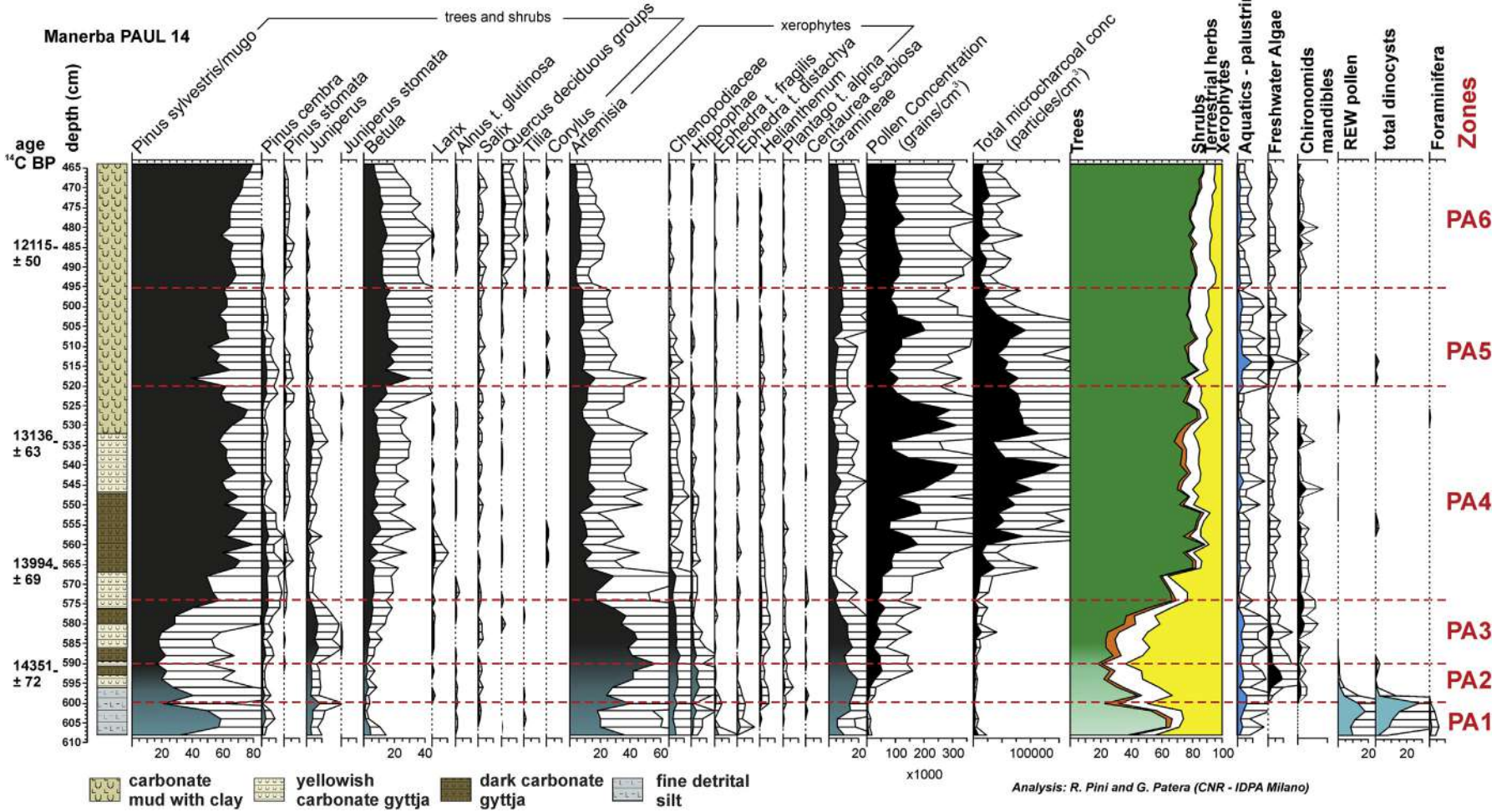

Fig. 10. Palynological record of selected species (%), summary concentrations of primary and secondary-deposited palynological items and of charcoal, plotted on stratigraphic scale. A blue/gray pattern filling marks high proportion of floated pollen while black fill is for airborne pollen. Magnification of percentage curves ×5. (For interpretation of the references to color in this figure legend, the reader is referred to the web version of this article.)

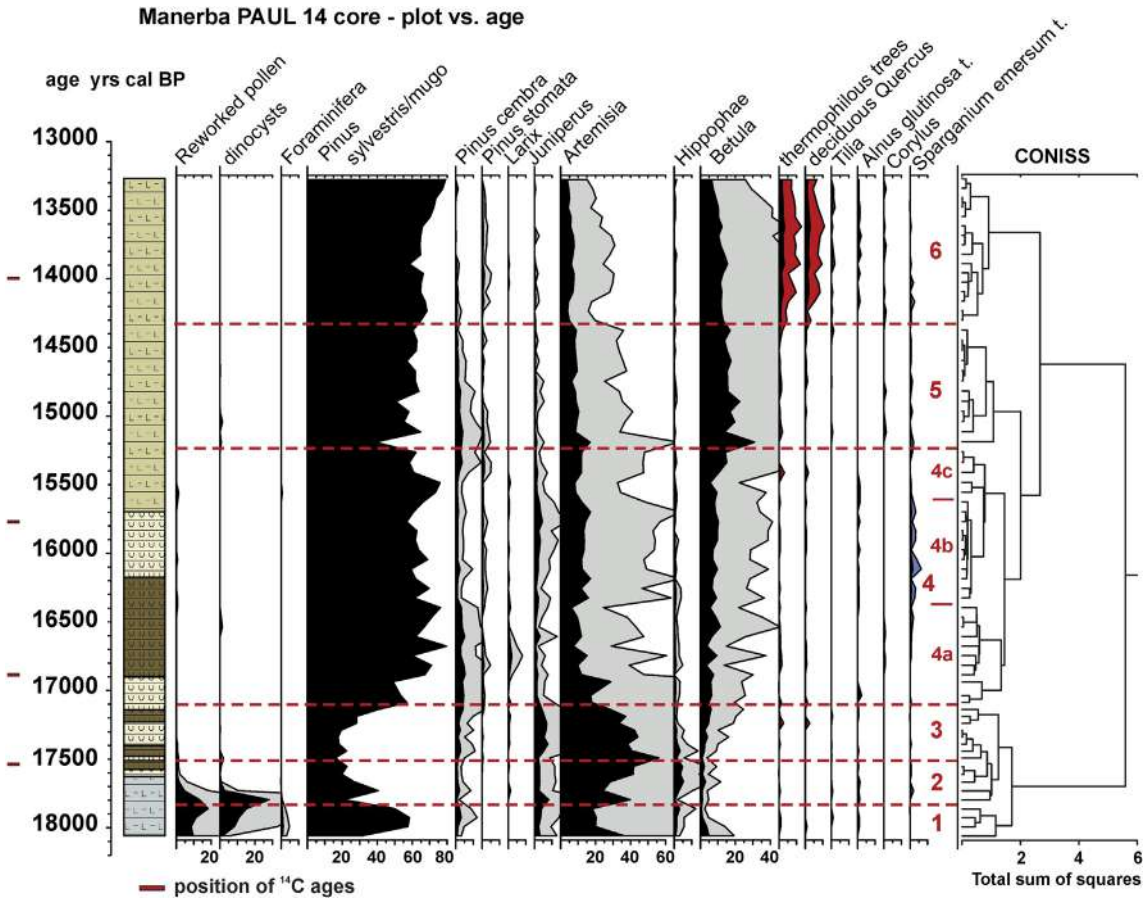

Fig. 11. Palynological record of most abundant *taxa* and of stomata, plotted on time scale. Thermophilous trees = sum of *Quercus, Tilia, Ulmus, Corylus*. Magnification of percentage curves ×5.

5.3. Timing of glacier collapse at the LGM end in the Garda Lake and in other overdeepened alpine basins

Given the stratigraphic and chronological constraints discussed in previous sections, the scenario for the last deglaciation of the Garda basin may be outlined as follows (Figs. 12–14).

5.3.1. LGM culminations

One or more culminations built the outer ridges of the moraine system after 32 ka cal BP, the glaciated Garda basin reaching up to 1242 km^2 (Figs. 12 and 14a). Analogous to sequences from other pedemontane end-moraine systems and their outwash at the Italian Alpine fringe (Fig. 1), these culmination phases may span from 27 to 21 ka cal BP (Monegato et al., 2007; Ravazzi et al., 2012; Mozzi et al., 2013; Rossato et al., 2013).

5.3.2. Late LGM oscillations

Several terminal arcs were added after the LGM culminations until the Manerba advance at 17.5 ka cal BP which is the last episode, with a glaciated surface of 677 km^2 (Fig. 14b). The Manerba advance represents the last readvance before the ultimate collapse and final withdrawal from the end-moraine system, thus it may be regarded as the event concluding the LGM south of the Alps.

5.3.3. Timing and history of the Manerba advance

The small and shallow lake selected for this study is located on an elevated bedrock pavement isolated from the hydrographic network since local deglaciation. At the deglacial onset, the hydrographic network over the promontory was suddenly deactivated due to decreasing level of the ice-contact paleo-Garda Lake. The spillouts feeding the small lake were diverted from the bedrock cliff threshold (120 m a.s.l.). This happened 17.55 ± 0.15 ka cal BP once the depletion of glacial meltwater supply in the continuous lake record is unambiguously shown by a fall in the record of reworked dinocysts marking the detrital supply from glacially abraded bedrock.

The age (17.4 ± 0.16) from a *Bison* skull (Figs. 3b and 4) represents the latest aggradation of the outwash supplied by western spillouts at exactly the same altitude (120 m a.s.l.). On this southwestern side of the promontory there is no bedrock threshold, thus the deglaciation left the outwash plain as a kame terrace hanging over the modern lake basin (Fig. 13b). Radiocarbon ages of late aggradation on one hill side and deglaciation on the other side are indistinguishable, thus there is no significant lag between them. The calibration of the mean pooled age from these dates (17.46 ± 0.2 ka cal BP, 17.23–17.66 ka cal BP, 2σ), provides a robust estimate for the onset of Lateglacial glacier collapse in the Garda basin (Fig. 14c). The relative glacial surface in the Garda basin is estimated 527 km^2.

5.3.4. The early Lateglacial collapse

Seismic profiles show no younger morainic ridges inward the Manerba end moraine. These circumstances suggest that the glacier body undertook a phase of pronounced downwasting after retreating from the Manerba advance, became stagnant and collapsed. The paleo-Garda Lake developed in front of it due to

Table 3
Summary of vegetation history and sedimentary environments at Manerba Paùl lake after deglaciation, 17.4 to 13.8 ka cal BP. m = median. yrs a.d. = years after deglaciation (median). See Table 2 for age probability intervals.

Depth PAUL 14	Events and phases in terrestrial vegetation	Littoral and aquatic vegetation and fauna	Sedimentation at the littoral studied site	Ecologic constrains to the aquatic / terrestrial systems	Inferred climate-stratigraphic trends and average climate	Chronology (m cal BP) and yrs a.d.
488–465	Mixed forest pine dominated	Tall herbs forming wet meadows in the telmatic belt	Grey micrite laminated carbonate mud. No reworking	Deep water	Suboceanic cool temperate	14.097–13.310 GI-1 interstadial
494–488	Thermophilous trees expansion					14.303–14.097 GI-1 interstadial
494	Onset of oak pollen, accompanied by *Alnus* t. *glutinosa* and *Tilia*			Lake level increase	Sharp warming and rainfall increase.	14.303–14.097 yrs a.d.=3362 (GI-1 onset)
526–494	Forest recovery around the lake, tree *Betula* expansion against pines. *Pinus cembra* late phase and desappearance from the lowlands	*Sparganium* decline, Cyperaceae (e.g. *Eriophorum*) and tall herbs expansion		Lake level increase / high frequency local forest fires	Warmer and wetter. Cold and wet temperate	15.486–14.303
552–526	*Pinus cembra* and *Larix* fall	*Sparganium emersum* type expansion, Chironomid mandibles reduction	Yellowish micrite carbonate, partly oxic sedimentation, sediment focusing testified by sporadic reworked palynomorphs (pollen and chitinous remains of Forams)	Littoral invaded by elophytic herbs, lake level fall (low stand) / several phases of peaking local forest fires	Persistently drier, colder and continental (1010-years duration event, "Ragogna oscillation"). Cold-temperate, continental	16.396–15.486 yrs a.d.= 1159–2069
558 (−555)	*Larix* fall, no significant forest opening	Onset *Sparganium emersum* type	Onset yellowish carbonates, partly oxic sedimentation	/ Forest fire frequency increase	Drier, continental	16.607 − 16.570
568–558	*Larix* expansion, dense pine-larch forest (AP 87–90%)	Abundant chironomid mandibles, especially in darker belts	Dark gyttja prevailing with micrite, anoxyc hypolimnion	Deep anoxic water / very low frequency forest fire	Wetter phase. Cold-temperate	16.950 − 16.607 yrs a.d.= 948
582–568	Massive afforestation (*Pinus sylvestris and Larix*)		Banded micrite carbonate mud with darker layers, anoxyc and productive hypolimnion	/ Low frequency forest fire		17.491 − 16.905 yr a.d.= 605
582	Woody vegetation start expanding around the lake			/ Charcoal particles increase over trend of pollen concentration	Warming	17.491 yrs a.d.= 64
596–582	Steppe and *Hippophaë-Juniperus* scrub around the lake, pioneer *P. sylvestris*, scettered. Pioneers*: Oxyria, Bupleurum, Linum austriacum* type	Blooms of green algae, mainly *Pediastrum integrum* and *Botryococcus*	Onset micrite carbonate precipitation, algal blooms-promoted	Cold, clean, oligotrophic, partly anoxic water		17.540–17.491
596				Meltwater supply ceases		17.555 yrs a.d.= 0
608–596	Poor information (Mostly floated pollen)	No aquatics, a few peat-forming macrophytes	Blue-gray meltwater laminated silt	Strong meltwater supply, Proglacial environment		

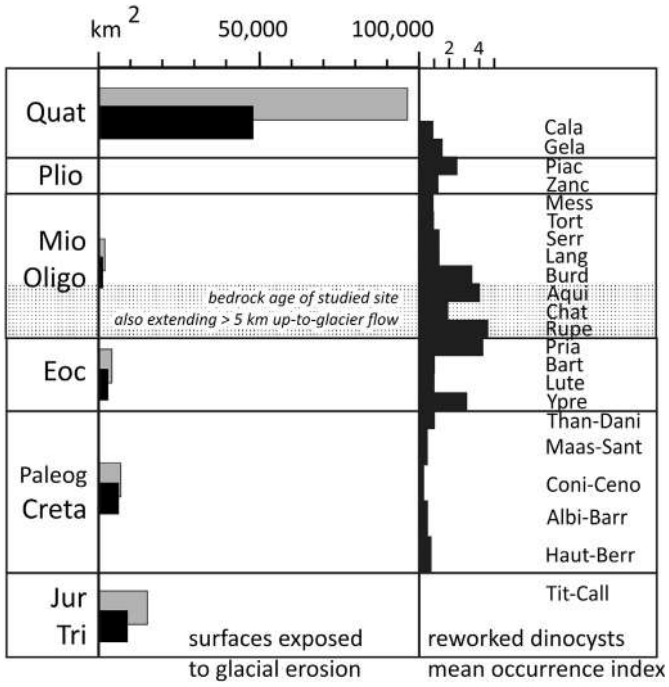

Fig. 12. Stratigraphically cumulated surfaces exposed to glacial abrasion in the Garda Lake basin (i.e. delimited north as in Fig. 2) computed for the culmination of LGM (left panel – gray bars) and of the Manerba advance (black bars). They are compared with the occurrence index of dinocysts reworked in meltwater silt in lake Paùl di Manerba (right panel). The area submerged today by the lake could not be computed. Its contribution to glacial abrasion is discussed in the text.

damming by the end-moraines and deposited varved sequences onlap to the slopehill belonging to the Manerba advance (Servizio Geologico d'Italia, 1969; see also; Baroni, 2010). This dynamics recalls the pattern described for Eastern Alps. Here, it was suggested that no readvance of the main glaciers occurred in the Lateglacial until alpine valley were free from dendritic glaciers (Reitner, 2007).

The timing of glacier withdrawal from the Garda Lake at the end of the Manerba advance fits the radiocarbon and cosmogenic chronologies for the withdrawal of the deep overdeepened basins hosting the foreland piedmont Alpine lakes both on the southern side of the Alps (Niessen and Kelts, 1989) and on the northern Swiss side (Lister, 1988; Hadorn et al., 2002; Ivy-Ochs et al., 2004, 2008). At the same time a significant glacial retreat is recorded both in the northern hemisphere (Giraudi and Frezzotti, 1997; Dyke et al., 2002) and on a nearly global scale, regardless to the expansion of sea ice in the North Atlantic during Heinrich Event 1 (Schaefer et al., 2006; Stanford et al., 2011).

A few ice-contact sequences from piedmont Alpine lakes provided even earlier radiocarbon ages. They result from lake inlets, terminal to the main foreland lake bodies (e.g. Lake Geneve, Moscariello et al., 1998; Lake Como, Comerci et al., 2007) and may be consistent with the deglacial sequence depicted in the present paper as they may derive from deposition beneath a calving ice margin. On the other hand, if the oldest available radiocarbon ages are taken as an evidence of deglaciation completed, then an earlier deglacial timing would be figured (i.e. swiss perialpine lakes ice-free at 20–19.2 ka cal BP, see Heiri et al., 2014 Fig. 6). Once more, it is safe excluding from this account ages deriving from bulk organic matter and/or with large uncertainties or from unidentified plant material of uncertain origin (e.g. Rödschitz, see van Husen, 1997). We also dropped any estimate of the deglacial lag, i.e. of the time period recorded by sediment deposited after local deglaciation and before the basal dated level.

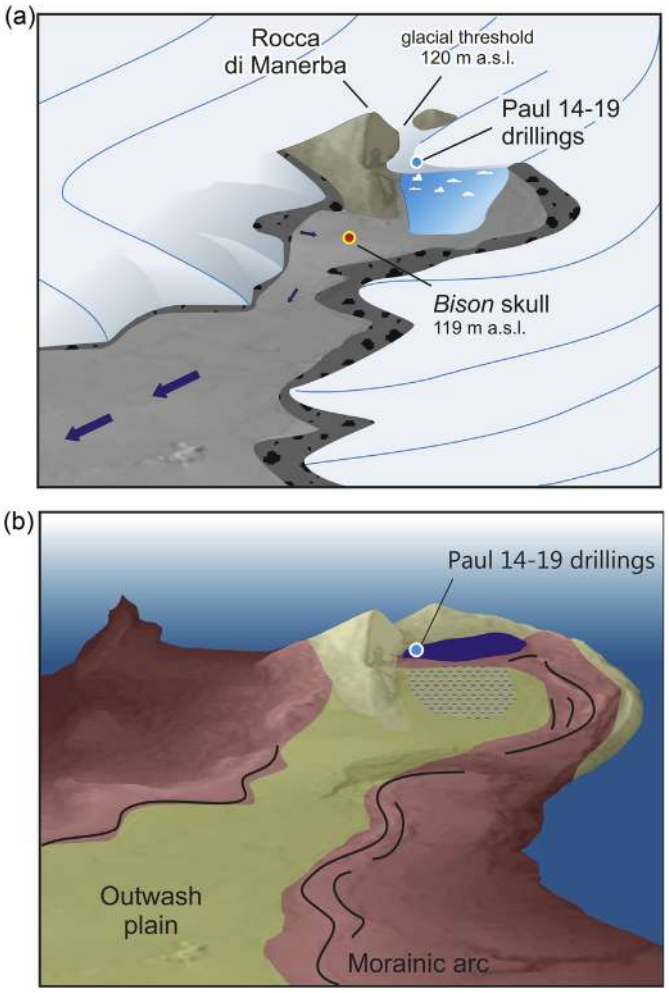

Fig. 13. 3D model reconstruction of the promontory of Manerba viewed from the South at the culmination of the Manerba advance (a) and after the glacier collapse (b).

5.4. *Effects of Heinrich Event 1 on a glacier forefield forest succession – the Ragogna oscillation*

The pollen record obtained from the Paùl lake shows a distinct primary ecological succession clearly driven by local deglaciation of the Manerba promontory. A sparse tree cover is detected about 160 modeled yrs after deglaciation, while a dense conifer forest was established about seven centuries after deglaciation. A similar successional pattern described from two other glacier forefields cleared from ice about 18–17.5 ka cal BP in the southeastern Italian Alps (Tagliamento end-moraine, Monegato et al., 2007; Oglio lateral end-moraine, Ravazzi et al., 2012). Despite considerable differences in forest composition related to biogeographical and regional climate gradients, a phase of rapid tree growth is detected at all these sites in the first millennium after deglaciation. Moreover, it is remarkable that in all three sites the late successional forest development is perturbed by a stage of forest recession, named "Ragogna oscillation" (Monegato et al., 2007). At Paùl di Manerba the litostratigraphic changes and spread of littoral vegetation provide evidence of decreased lake level. These data speak for decreased runoff, and exclude a local trigger by fluvial or slope activity. Instead, duration and stability of pollen curves for about a millennium point to a climate trigger, likely a millennial phase of cooler-continental conditions marked by the Heinrich event style, with a sudden onset and end (Bond et al., 1997). After collapse of

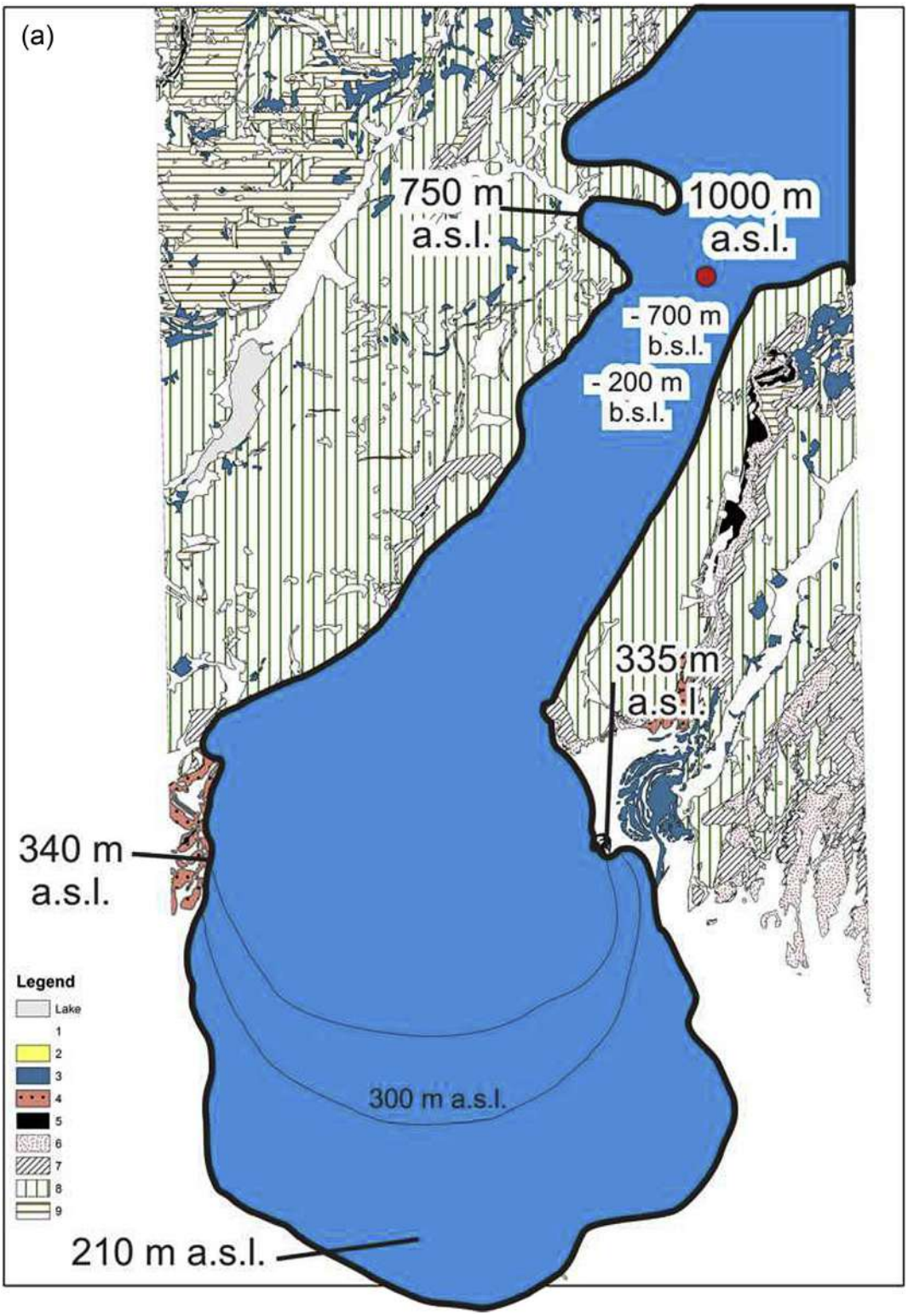

Fig. 14. Evolution of the ice-contact lake paleo-Garda. (a) Maximum extent of the Garda glacier lobe during the Last Glacial Maximum, selected contour lines and spot elevations of glacier surface (after Habbe, 1969; Castellarin et al., 2005); (b) Manerba advance culmination; (c) early collapse and ice-contact lake formation.

pedemontane glacial lobes at around 17.5 ka cal BP, glacier activity remained confined into Alpine valleys, well upstream of foreland prealpine lakes (Kerschner et al., 1999; Ivy-Ochs et al., 2006), thus glacial advances may not be directly responsible for the observed changes in a closed lake, isolated from the main hydrographic network. However it is likely that such a triggering climate event also drove glacier advances upstream in the valleys. At Manerba this cold-continental event is framed between modeled ages 16,395 ± 160 and 15,480 ± 160 yrs cal BP, that fit the Gschnitz stadial timing (Ivy-Ochs et al., 2006) and its paleoclimate

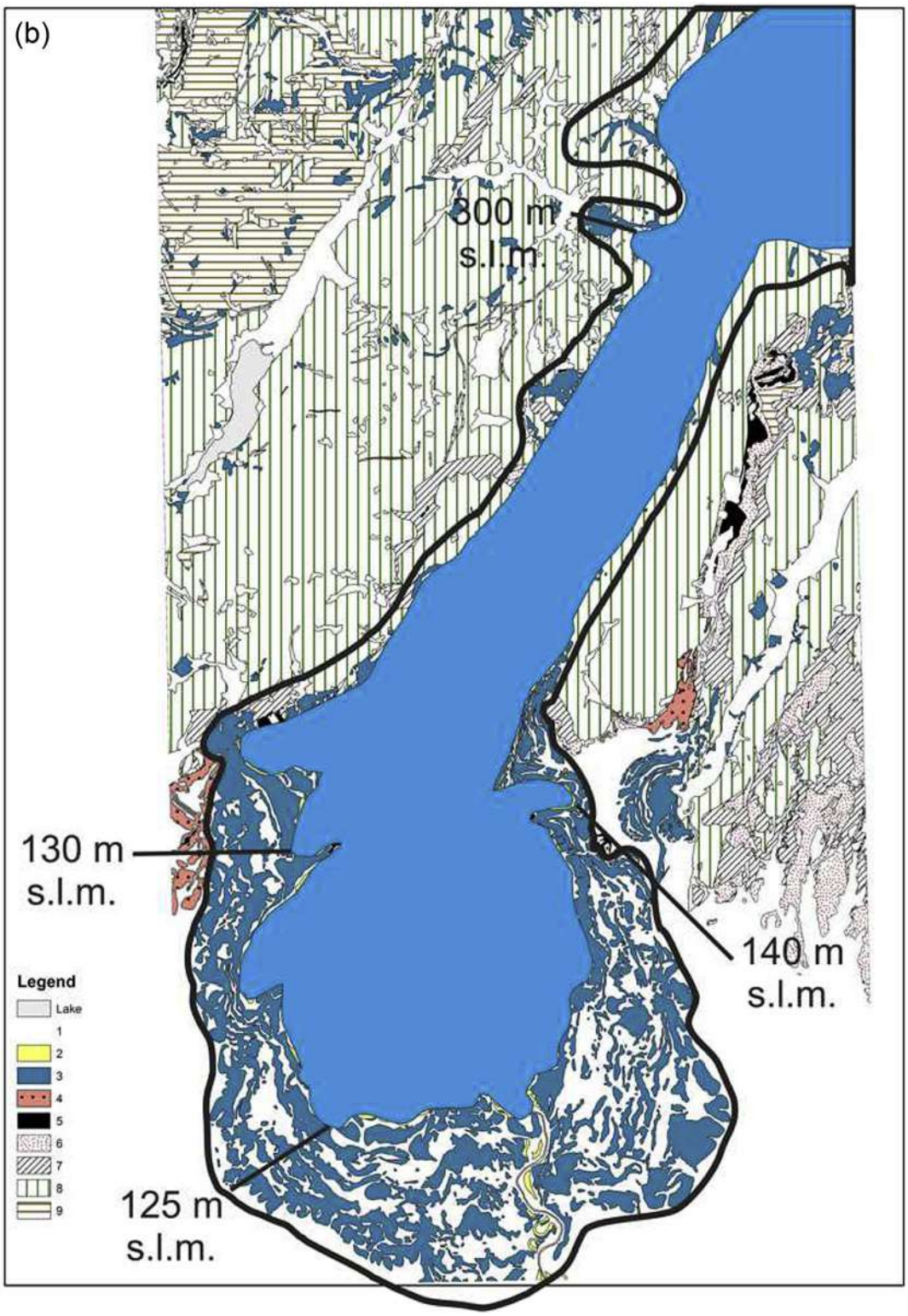

Fig. 14. (*continued*).

reconstruction (Kerschner and Ivy-Ochs, 2007), thus spanning the most advanced phase of Heinrich Event 1 (Stanford et al., 2011). The impact on forest and herb vegetation is moderate, and might not be apparent from pollen changes in treeless regions of the Alps and central Europe. This latter argument provides a possible explanation for missed detection of the Ragogna oscillation in pollen records north of the Alps.

6. Conclusions

A comparative multidisciplinary study in Quaternary geology, lake paleoecology, marine microfossils and vertebrate palaeontology gave new insight about timing and history of the glacial sequence ending the Last Glacial Maximum in the largest end-moraine system at the fringe of the Italian Alps (the Garda glacial

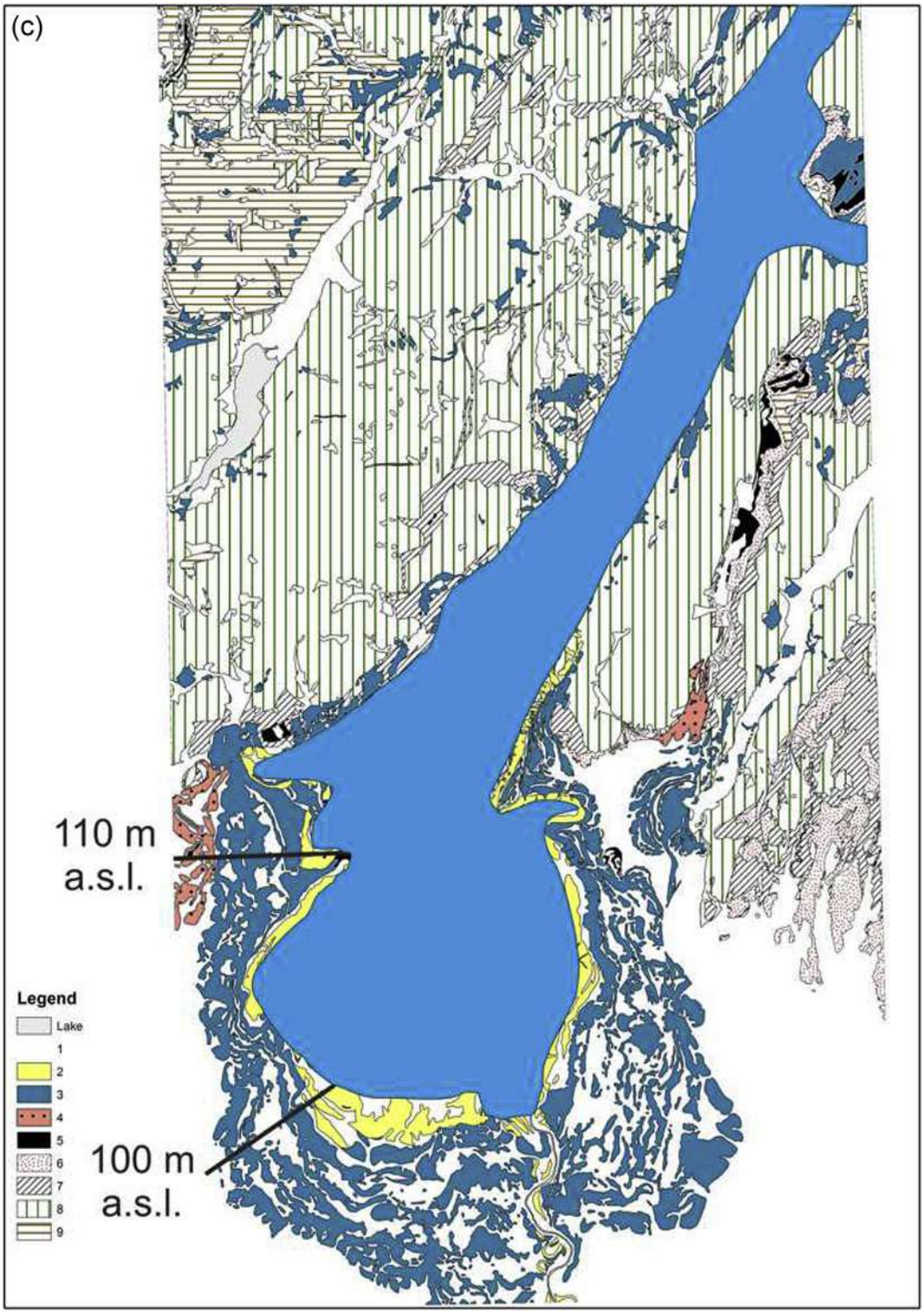

Fig. 14. (*continued*).

amphitheatre). The ecosystem response to these dramatic changes could also be detected at a time resolution (50–70 yrs) comparable to the steps of vegetation chronosequence in deglaciated forefields.

The issue of stratigraphically detecting the local deglaciation in proglacial lake records was successfully achieved by analyzing dinocysts reworked by glacial abrasion from marine bedrock. Dinocysts trace the age source of glacial abrasion and depict the stratigraphic record of meltwater silt versus autochtonous sedimentation in the deglacial sequence. Cross-radiocarbon dating of the deglacial lake sequence and of the activity of the outwash aggradation allowed an independent checking of the local deglaciation time frame.

The ultimate glacier collapse and final withdrawal of the deep overdeepened basin hosting the Garda Lake started 17.46 ± 0.2 ka

cal BP, after the last LGM culmination. This deglaciation timing appears to be synchronous at millennial scale, with several foreland piedmont lakes both on southern and northern sides of the Alps and with large-scale glacial retreat at global scale.

The "Ragogna oscillation", an early Lateglacial millennial event of forest recession so far known from two glacier forefields in SE-Alps, is confirmed by evidence of a stage of forest recession in the deglacial lake record, and here dated from 16.4 ± 0.16 to 15.5 ± 0.16 yrs cal BP. The well-known Gschnitz stadial glacier advance is believed to have been triggered by the same millennial north-Atlantic events, during the advanced phases of Heinrich Event 1.

The early Lateglacial history of Alpine geoecosystems provides the prerequisite to understand the subsequent dramatic changes associated with the last glacial–interglacial transition. Hence, further ecosystem and climate proxies deserve high-resolution analysis from the intermorainic lake deglacial sequences preserved in the end moraine systems of the Alps.

Acknowledgments

We are indebted to the Municipality of Manerba del Garda and to Soprintendenza per i Beni Archeologici della Lombardia, who promoted drillings in the Lake Paùl di Manerba. Dr. C. Mangani (Museo Archeologico "G. Rambotti", Desenzano del Garda), dr. B. Portulano (Museo di Manerba del Garda) and prof. B. Sala (University of Ferrara) provided assistance during coring and sampling operations for radiocarbon dating. We acknowledge the many people helping during field work. The results of this study could not be achieved without skilful technical borehole by Fabio Baio (Villa d'Adda, Bergamo). This paper is a contribution to the research Line C.N.R. - DPA, TA.P02.005 "Evoluzione geologica, cambiamenti ambientali e climatici nel Quaternario e mutue interazioni con le civiltà".

Appendix A. Locations of boreholes and open sections examined and mentioned (coordinates obtained from Google Earth)

Manerba advance

Site 1 – Soil profile Sasso di Manerba, 132 m a.s.l.. 45°33′29.45″N; 10°34′31.87″E.

Site 3 – Bison skull location, Crociale di Manerba, 118 m a.s.l.. 45°32′48.40″N; 10°32′50.63″E.

Paùl di Manerba boreholes

PAUL 14, 123 m a.s.l. – 45°33′23.39″N; 10°34′22.06″E.

PAUL 19, 123 m a.s.l. – 45°33′23.20″N; 10°34′22.30″E.

Sites correlated to the Manerba advance

Soil profile at the moraine hilltop East of the Lavagnone basin, 115 m a.s.l. – 45°26′14.96″N; 10°32′29.00″E.

Lateglacial cores from the Lavagnone basin, 103 m a.s.l., 45°26′11.15'' N; 10°32′14.06″E.

Lake Frassino, 72 m a.s.l., 45°26′12.45″N; 10°39′56.16″E.

LGM stages

Val Sorda succession, 280 m a.s.l. – 45°32′57.69″N; 10°45′24.14″E.

Appendix B. Identification of reworked items, pollen, non pollen palynomorphs and stomata

Identification of reworked items

(i) Pre-Quaternary palynomorphs are poorly preserved and show an enhanced thermal maturation; (ii) Pre-Quaternary marine dinoflagellates must originate from glacially-abraded marine sediments; (iii) Co-variation between abundance of unidentifiable pollen, marine dinoflagellates and foraminiferal linings suggests a common origin for these items. These criteria may provide a reliable method when marine sedimentary rocks occur in the basin catchment (i.e. Pini et al., 2009).

Identification of pollen, non pollen palynomorphs and stomata

Reference literature: Trautmann, 1953; Punt et al., 1976–2009; van Geel et al., 1983, and 1989; Reille, 1992–1998; Komárek and Jankovska, 2001; Reille, 1992–1998; Streble and Krauter, 2002; Beug, 2004. Nomenclature of pollen types follows Beug (2004).

Identification of Pinus sylvestris/mugo and P. cembra pollen and stomata

Identification of *P. sylvestris/mugo* and of *P. cembra* pollen was based on *sacci* morphology, their connection to the grain body and the absence/presence of *pustulae* on the ventral portion of the grain (Moore et al., 1991; Pini et al., 2009).

Stomata were identified according to criteria so far used to identify conifer and Mediterranean pines stomata (Sweeney, 2003; García Álvarez et al., 2009).

Appendix A. Supplementary data

Supplementary data related to this article can be found at http://dx.doi.org/10.1016/j.quascirev.2014.09.014.

References

Accorsi, C.A., Aitken, M.J., Cremaschi, M., Ferraris, M., McElroy, C., Questiaux, D., Van Vliet Lanoe, B., 1990. The loess deposits of the Rivoli moraine system. In: Cremaschi, M. (Ed.), The Loess in Northern and Central Italy. A Loess Basin between the Alps and the Mediterranean Region, vol. 1. CNR, Quaderni di Geodinamica Alpina e Quaternaria, Milano, pp. 21–39.

Alberti, G., 1961. Zur Kenntnis Mesozoischen und Alttertiärer Dinoflagellaten und Hystrichosohaerideen von Nord-und Mitteldeutschland sowie einigen anderen europäischen Gebieten. Palaeontogr. Abt. A Stuttg. 116, 1–58.

Ammann, B., 1994. Differential flotation of saccate pollen – a nuisance and a chance. Diss. Bot. 234, 101–110.

Ammann, B., van Raden, U.J., Schwander, J., Eicher, U., Gilli, A., Bernasconi, S.M., van Leeuwen, J.F.N., Lischke, H., Brooks, S.J., Heiri, O., Nováková, K., van Hardenbroek, M., von Grafenstein, U., Belmecheri, S., van der Knaap, W.O., Magny, M., Eugster, W., Colombaroli, D., Nielsena, E., Tinner, W., Wright, H.E., 2013. Responses to rapid warming at Termination 1a at Gerzensee (Central Europe): primary succession, albedo, soils, lake development, and ecological interactions. Palaeogeogr. Palaeoclimatol. Palaeoecol. 391, 111–131.

Ammann, B., van der Knaap, W.O., Lang, G., Gaillard, M.J., Kaltenrieder, P., Rösch, M., Finsinger, W., Wright, H.E., Tinner, W., 2014. The potential of stomata analysis in conifers to estimate presence of conifer trees: examples from the Alps. Veget. Hist. Archaeobot. 23, 249–264.

Arpenti, E., Ravazzi, C., Deaddis, M., 2004. Il Lavagnone di Desenzano del Garda: analisi pollinica e informazioni paleoecologiche sui depositi lacustri durante le prime fasi d'impianto dell'abitato (Antica età del Bronzo). Not. Archeol. Bergomensi 10 (2002), 35–54.

Baroni, C., 2010. Paleolivelli tardoglaciali e olocenici del Lago di Garda. In: Orombelli, G., Cassinis, G., Gaetani, M. (Eds.), Una nuova geologia per la Lombardia. Istituto Lombardo – Accademia di Scienze e Lettere, pp. 231–254.

Baroni, C., Cremaschi, M., 1987. Geologia e pedostratigrafia della collina di Ciliverghe (Brescia). Nat. Brescia. 23, 55–78.

Baroni, C., Vercesi, P.L., 1995. Note Illustrative della Carta Geologica delle Prealpi Bresciane Tra La Val Vrenda e il M. Pizzocolo. Atti Ticinensi Sci. della Terra 38, 65–93.

Baroni, C., Zanchetta, G., Fallick, A.E., Longinelli, A., 2006. Mollusca stable isopote record of a core from Lake Frassino, northern Italy: hydrological and climatic changes during the last 14 ka. Holocene 16 (6), 827–837.

Bennett, M.R., Glasser, N.F., 1996. Glacial Geology. Ice Sheets and Landforms. Wiley & Sons, Chichester, p. 364.

Bertoldi, R., 1968. Ricerche polliniche sullo sviluppo della vegetazione tardiglaciale e postglaciale nella regione del lago di Garda. Stud. Trent. Sci. Nat., sez. B 45 (1), 87–162.

Beug, H.J., 2004. Leitfaden der Pollenbestimmung für Mitteleuropa und angrenzende Gebiete. Verlag Dr. Friedrich Pfeil, München.

Bini, A., Zuccoli, L., 2004. Prime note sul rilevamento dell'anfiteatro del Garda: metodi e unità provvisorie. Il Quat. 17, 333–342.

Bond, G., Showers, W., Cheseby, M., Lotti, R., Almasi, P., deMenocal, P., Priore, P., Cullen, H., Hajdas, I., Bonani, G., 1997. A pervasive millennial-scale cycle in North Atlantic Holocene and glacial climates. Science 278, 1257–1266.

Boulton, G.S., 1979. Processes of glacier erosion on different substrata. J. Glaciol. 23 (89), 15–38.

Bronk Ramsey, C., 2008. Deposition models for chronological records. Quat. Sci. Rev. 27, 42–60.

Bruhn, F., Duhr, A., Grootes, P.M., Mintrop, A., Nadeau, M.J., 2001. Chemical removal of conservation substances by 'soxhlet'-type extraction. Radiocarbon 43 (2A), 229–237.

Cadrobbi, M., Pasa, A., Trevisan, L., 1948. Foglio 35 Riva. Carta Geologica delle Tre Venezie. Magistrato delle Acque, Venezia.

Callegari, E., Dal Piaz, G., Gatto, G.O., 2002. Carta geologica del gruppo Adamello-Presanella. Consiglio Nazionale delle Ricerche, Selca, Firenze.

Castellarin, A., Cantelli, L., 2000. Neo-Alpine evolution of the southern eastern alps. J. Geodyn. 30, 251–274.

Castellarin, A., Picotti, V., Cantelli, L., Claps, M., Trombetta, L., Selli, L., Carton, A., Borsato, A., Daminato, F., Nardin, M., Santuliana, E., Veronese, L., Bollettinari, G., 2005. Note illustrative della Carta Geologica d'Italia alla scala 1:50.000. Foglio 080 Riva del Garda. APAT, Roma.

Castiglioni, B., 1940. L'Italia nell'Età Quaternaria. In: Atlante Fisico D'Italia. Touring Club Italiano, Milano. Map at scale 1:200.000.

Comerci, V., Cappelletti, S., Michetti, A.M., Rossi, S., Serva, L., Vittori, E., 2007. Land subsidence and lateglacial environmental evolution of the Como urban area (Northern Italy). Quat. Int. 173–174, 67–86.

Cremaschi, M., 1987. Paleosols and Vetusols in the Central Po Plain (Northern Italy). Unicopli, Milano.

Curzi, P.V., Castellarin, A., Ciabatti, M., Badolini, G., 1992. Caratteri morfostrutturali sedimentologici e genetici del Lago di Garda. Boll. Soc. Torricelliana Sci. Lett. Faenza 43, 3–111.

D'Amico, M.E., Freppaz, M., Filippa, G., Zanini, E., 2014. Vegetation influence on soil formation rate in a proglacial chronosequence (Lys Glacier, NW Italian Alps). Catena 113, 122–137.

Dean, W.E., 1974. Determination of carbonate and organic matter in calcareous sediments and sedimentary rocks by loss on ignition: comparison with other methods. J. Sed. Petrol. 44, 242–248.

Dean, W.E., 1999. The carbon cycle and biogeochemical dynamics in lake sediments. J. Paleolimnol. 21, 375–393.

Dean, W.E., Fouch, T.D., 1983. Lacustrine environment. In: Scholle, P.A., Bebout, D.G., Moore, C.H. (Eds.), Carbonate Depositional Environments. AAPG, Oklahoma, USA.

De Coninck, J., 1975. Microfossiles à paroi organique de l'Yprésien du bassin belge. – Administration des mines – Service géologique de Belgique. Prof. Pap. Brux. 12, 1–151.

Dyke, A.S., Andrews, J.T., Clark, P.U., England, J.H., Miller, G.H., Shaw, J., Veillette, J.J., 2002. The Laurentide and Innuitian ice sheets during the last glacial maximum. Quat. Sci. Rev. 21, 9–31.

Eyles, N., Menzies, J., 1983. The subglacial landsystem. In: Eyles, N. (Ed.), Glacial Geology. Pergamon Press, Oxford, pp. 19–70.

ERSAL, 1997. I Suoli Dell'area Morenica Gardesana, p. 170. Settore bresciano. Regione Lombardia, Milano.

Ferraro, F., 2009. Age, sedimentation, and soil formation in the Val Sorda loess sequence, Northern Italy. Quat. Int. 204, 54–64.

Fisher, T.G., Waterson, N., Lowell, T.V., Hajdas, I., 2009. Deglaciation ages and meltwater routing in the Fort McMurray region, northeastern Alberta and northwestern Saskatchewan, Canada. Quat. Sci. Rev. 28, 1608–1624.

García Álvarez, S., Morla Juaristi, C., Solana Gutiérrez, J., García-Amorena, I., 2009. Taxonomic differences between *Pinus sylvestris* and *P. uncinata* revealed in the stomata and cuticle characters for use in the study of fossil material. Rev. Palaeobot. Palynol. 155, 61–68.

Geel, B., van, Hallewas, D.P., Pals, J.P., 1983. A late Holocene deposit under the Westfries Zeedijk near Enkhuizen (prov. of Noord-Holland, The Netherlands): palaeoecological and archaeological aspects. Rev. Palaeobot. Palynol 38, 269–335.

Geel, B., van, Coope, G.R., van der Hammen, T., 1989. Palaeoecology and stratigraphy of the Lateglacial type section at Usselo (The Netherlands). Rev. Palaeobot. Palynol 60, 25–129.

Gile, L.H., Peterson, F.F., Grossman, R.B., 1966. Morphological and genetic sequences of carbonate accumulation in desert soils. Soil Sci. 101 (5), 347–360.

Giraudi, C., Frezzotti, M., 1997. Late Pleistocene glacial events in the central Apennines, Italy. Quat. Res. 48, 280–290.

Grimm, E.C., 1987. CONISS: a FORTRAN 77 program for stratigraphically constrained cluster analysis by the method of incremental sum of squares. Comput. Geosci. 13 (1), 13–35.

Grimm, E.C., 1991-2011. Tilia 1.7.16. Illinois State Museum, Research and Collection Center, Springfield.

Grüger, J., 1968. Untersuchungen zur spätglazialen und frühpostglazialen Vegetationsentwicklung der Südalpen im Umkreis des Gardasees. Bot. Jahrb. Syst. Pflanzengesch. Pflanzengeogr 88, 163–199.

Habbe, K.A., 1969. Die würmzeitliche Vergletscherung des Gardasee-Gebietes. In: Freiburger Geographische Arbeiten, vol. 3.

Hadorn, P., Thew, N., Coope, G.R., Lemdahl, G., Hajdas, I., Bonani, G., 2002. A Late-Glacial and early Holocene environment and climate history for the Neuchâtel region (CH). In: Richard, H., Vignot, A. (Eds.), Equilibres et ruptures dans les eccosystemes depuis 20000 ans en Europe de l'Ouest, Collection Annales Litte'raires, Série Environment, Sociétés et Archéologie, vol. 3, pp. 75–90.

Hakanson, L., Jansson, M., 1983. Principles of Lake Sedimentology. Springer, Berlin, p. 332.

Hallet, B., 1976. The effect of subglacial chemical processes on glacier sliding. J. Glaciol. 17, 209–221.

Heiri, O., Koinig, K.A., Spötl, C., Barrett, S., Brauer, A., Drescher-Schneider, R., Gaar, D., Ivy-Ochs, S., Kerschner, H., Luetscher, M., Moran, A., Nicolussi, K., Preusser, F., Schmidt, R., Schoeneich, P., Schwörer, C., Sprafke, T., Terhost, B., Tinner, W., 2014. Palaeoclimate records 60–8 ka in 1 the Austrian and Swiss Alps and their forelands (in press). Quat. Sci. Rev.. http://dx.doi.org/10.1016/j.quascirev.2014.05.021.

Holzhauser, H., 2010. Zur Geschichte des Gornergletschers. Ein Puzzle aus historischen Dokumenten und fossilen Hölzern aus dem Gletschervorfeld. In: Geographica Bernensia, vol. 84. Geographisches Institut der Universität Bern, Bern.

Hormes, A., Müller, B.U., Schlüchter, C., 2001. The Alps with little ice: evidence for eight Holocene phases of reduced glacier extent in the Central Swiss Alps. Holocene 11 (3), 255–265.

Ivy-Ochs, S., Schäfer, J., Kubik, P.W., Synal, H.-A., Schlüchter, C., 2004. Timing of deglaciation on the northern Alpine foreland (Switzerland). Eclogae Geol. Helv. 97, 47–55.

Ivy-Ochs, S., Kerschner, H., Kubik, P.W., Schlüchter, C., 2006. Glacier response in the European Alps to Heinrich Event 1 cooling: the Gschnitz stadial. J. Quat. Sci. 21 (2), 115–130.

Ivy-Ochs, S., Kerschner, H., Reuther, A., Preusser, F., Hiene, K., Maisch, M., Kubik, P.W., Schlüchter, C., 2008. Chronology of the last glacial cycle in the European Alps. J. Quat. Sci. Rev. 23 (6–7), 559–573.

Kaiser, K.F., Friedrich, M., Miramont, C., Kromer, B., Sgier, M., Schaub, M., Boeren, I., Remmele, S., Talamo, S., Guibal, F., Sivan, O., 2012. Challenging process to make the Lateglacial tree-ring chronologies from Europe absolute – an inventory. Quat. Sci. Rev. 36, 78–90.

Kelts, K., Hsü, K.J., 1978. Freshwater carbonate sedimentation. In: Lerman, A. (Ed.), Lakes. Chemistry, Geology, Physics. Springer, New York.

Kerschner, H., Ivy-Ochs, S., Schlüchter, C., 1999. Paleoclimatic intepretation of the early late-glacial in the Gschnitz valley, Central Alps, Austria. Ann. Glaciol. 28, 135–140.

Kerschner, H., Ivy-Ochs, S., 2007. Palaeoclimate from glaciers: examples from the Eastern Alps during the Alpine Lateglacial and early Holocene. Glob. Planet. Change 60, 58–71.

Komárek, J., Jankovska, V., 2001. Review of the Green Algal Genus *Pediastrum*. Implication for Pollen – Analytical Research. In: Biblioteca Phycologica, 108 (Stuttgart).

Kukal, Z., 1971. Geology of Recent Sediments. Academic Press, London, p. 490.

Lambeck, K., Yokoyama, Y., Purcell, T., 2002. Into and out of the Last Glacial Maximum: sea-level change during Oxygen Isotope Stage 3 and 2. Quat. Sci. Rev. 21, 343–360.

Lister, G., 1988. A 15,000 Year isotopic record from lake Zürich of Deglaciation and Climatic Change in Switzerland. Quat. Res. 29, 129–141.

Mancini, F., 1969. Notizie sui paleosuoli e sui loess dell'anfiteatro occidentale e frontale del Garda. Atti Soc. Ital. Sci. Nat. Mus. Civ. Storia Nat. Milano 100 (2), 185–210.

Manum, S.B., Boulter, M.C., Gunnarsdottir, H., Rangnes, K., Scholze, A., 1989. Eocene to miocene palynology of the Norvegian sea (ODP Leg 104). In: Eldholm, O., Thiede, J., Taylor, E. (Eds.), Proceedings of the Ocean Drilling Program, Scientific Results, vol. 104, pp. 611–662.

Matthews, J.A., 1992. The Ecology of Recently-deglaciated Terrain. Cambridge University Press, Cambridge.

Monegato, G., Ravazzi, C., Donegana, M., Pini, R., Calderoni, G., Wick, L., 2007. Evidence of a two-fold glacial advance during the Last Glacial Maximum in the Tagliamento end moraine system (SE Alps). Quat. Res. 68, 284–302.

Moore, P.D., Webb, J.A., Collinson, M.E., 1991. Pollen Analysis. Blackwell Scientific Publications. Oxford University Press.

Moreau, M., Mercier, D., Laffly, D., Roussel, E., 2008. Impacts of recent paraglacial dynamics on plant colonization: a case study on Midtre Lovénbreen foreland, Spitsbergen (79°N). Geomorphology 95, 48–60.

Moscariello, A., Pugin, A., Wildi, W., Beck, C., Chapron, E., de Batist, M., Girardclos, S., Ivy-Ochs, S., Rachoud-Schneider, A.-M.-, Signer, C., Clauwenberghe, T., 1998. Déglaciation würmienne dans des conditions lacustres à la termination occidentale du bassin lémanique (Suisse occidentale et France). Eclogae Geol. Helv. 91, 185–201.

Mozzi, P., Ferrarese, F., Fontana, A., 2013. Integrating digital elevation models and stratigraphic data for the reconstruction of the post-LGM unconformity in the Brenta alluvial megafan (north-eastern italy). Alp. Mediterr. Quat. 26 (1), 41–54.

Niessen, F., Kelts, K., 1989. The deglaciation and Holocene sedimentary evolution of southern perialpine Lake Lugano – implications for Alpine paleoclimate. Eclogae Geol. Helv. 82 (1), 235–263.

Nováková, K., van Hardenbroek, M., van der Knaap, W.O., 2013. Response of subfossil Cladocera in Gerzensee (Swiss Plateau) to early Late Glacial environmental change. Palaeogeogr. Palaeoclimatol. Palaeoecol. 391, 84–89.
Penck, A., Brückner, E., 1909. Die Alpen im Eiszeitalter, vol. 3, p. 1199.
Pini, R., Ravazzi, C., Donegana, M., 2009. Pollen stratigraphy, vegetation and climate history of the last 215 ka in the Azzano Decimo core (plain of Friuli, northeastern Italy). Quat. Sci. Rev. 28, 1268–1290.
Preusser, F., Reitner, J.M., Schlüchter, C., 2010. Distribution, geometry, age and origin of overdeepened valleys and basins in the Alps and their foreland. Swiss J. Geosci. 103, 407–426.
Punt, W., Blackmore, S. (Eds.), 1976–2009. The Northwest European Pollen Flora. vol. I–IX. Elsevier Publishing Company.
Rasband, W.S., 1997-2014. ImageJ. U. S. National Institutes of Health, Bethesda, Maryland, USA. http://imagej.nih.gov/ij/.
Ravazzi, C., Badino, F., Marsetti, D., Patera, G., Reimer, P.J., 2012. Glacial to paraglacial history and forest recovery in the Oglio glacier system (Italian Alps) between 26 and 15 kyr cal BP. Quat. Sci. Rev. 58, 146–161.
Reille, M., 1992-1998. Pollen et spores d'Europe et d'Afrique du nord, vol. 1 (Suppl. I–II). Faculté S. Jerome, Université de Marseille, Marseille.
Reimer, P.J., Bard, E., Bayliss, A., Beck, J.W., Blackwell, P.G., Bronk Ramsey, C., Buck, C.E., Cheng, H., Edwards, R.L., Friedrich, M., Grootes, P.M., Guilderson, T.P., Haflidason, H., Hajdas, I., Hatté, C., Heaton, T.J., Hogg, A.G., Hughen, K.A., Kaiser, K.F., Kromer, B., Manning, S.W., Niu, M., Reimer, R.W., Richards, D.A., Scott, E.M., Southon, J.R., Turney, C.S.M., van der plicht, J., 2013. IntCal13 and MARINE13 radiocarbon age calibration curves 0–50,000 years cal BP. Radiocarbon 55 (4), 1869–1887.
Reitner, J., 2007. Glacial dynamics at the beginning of Termination I in the Eastern Alps and their stratigraphic implications. Quat. Int. 164–165, 64–84.
Rossato, S., Monegato, G., Mozzi, P., Cucato, M., Gaudioso, B., Miola, A., 2013. Late Quaternary glaciations and connections to the piedmont plain in the prealpine environment: the middle and lower Astico Valley (NE Italy). Quat. Int. 288, 8–24.
Schaefer, J.M., Denton, G.H., Barrell, D.J.A., Ivy-Ochs, S., Kubik, P.W., Andersen, B.G., Phillips, F.M., Lowell, T.V., Schlüchter, C., Schaefer, 2006. Near-synchronous Interhemispheric termination of the last glacial maximum in Mid-Latitudes. Science 312, 1510–1513.
Schmidt, R., Weckstrom, K., Lauterbach, S., Tessadri, R., Huber, K., 2012. North Atlantic climate impact on early late-glacial climate oscillations in the south eastern Alps inferred from a multi-proxy lake sediment record. J. Quat. Sci. 27, 40–50.
Schnurrenberger, D., Russell, J., Kelts, K., 2003. Classification of lacustrine sediments based on sedimentary components. J. Palaeolimnol. 29, 141–154.
Sercelj, A., 1996. The Origins and Development of Forests in Slovenia. In: Academia Scientiarum et Artium Slovenica, Classis IV. Dela Opera, vol. 35, pp. 1–142.
Servizio Geologico d'Italia, 1969. Note Illustrative Alla Carta Geologica D'Italia Alla Scala 1:100.000, p. 95. Foglio 48-Peschiera del Garda. Napoli.
Sharp, M., Tranter, M., Brown, G.H., Skidmore, M., 1995. Rates of chemical denudation and CO_2 drawdown in a glacier-covered alpine catchment. Geology 23, 61–64.
Stanford, J.D., Rohling, E.J., Bacon, S., Roberts, A.P., Grousset, F.E., Bolshawa, M., 2011. A new concept for the paleoceanographic evolution of Heinrich event 1 in the North Atlantic. Quat. Sci. Rev. 30, 1047–1066.
Streble, H., Krauter, D., 2002. Atlante dei microrganismi acquatici. Franco Muzzio Editore 333.
Stockmarr, J., 1971. Tablets with spores used in absolute pollen analysis. Pollen Spores 13, 615–621.
Sweeney, C.A., 2003. A key for the identification of stomata of the native conifers of Scandinavia. Rev. Palaeobot. Palynol. 128, 281–290.
Talbot, M.R., Allen, P.A., 1996. Lakes. In: Reading, H.G. (Ed.), Sedimentary Environments: Processes, Facies and Stratigraphy, third ed. Blackwell Science, Oxford.
Toivonen, H., Huttunen, P., 1995. Aquatic macrophytes and ecological gradients in 57 small lakes in southern Finland. Aquat. Bot. 51, 197–221.
Trautmann, W., 1953. Zur Unterscheidung fossiler Spaltöffnungen der mitteleuropäischen Coniferen. Flora 140, 523–533.
Valsecchi, V., Tinner, W., Finsinger, W., Ammann, B., 2006. Human impact during the Bronze Age on the vegetation at Lago Lucone (northern Italy). Veget. Hist. Archaeobot 15, 99–113.
van Husen, D., 1997. LGM and Late-glacial fluctuations in the Eastern Alps. Quat. Int. 38/39, 109–118.
Van Simaeys, S., Brinkhuis, H., Pross, J., Williams, G.L., Zachos, J.C., 2005. Arctic dinoflagellate migrations mark the strongest Oligocene glaciations. Geology 33 (9), 709–712.
Venzo, S., 1957. Rilevamento geologico dell'anfiteatro morenico del Garda. Parte I: tratto occidentale Gardone – Desenzano. Mem. Soc. Ital. Sci. Nat. 12 (2), 1–140.
Venzo, S., 1965. Rilevamento geologico dell'anfiteatro morenico frontale del Garda dal Chiese all'Adige. Mem. del Mus. civico Storia Nat. Milano 14 (1), 82 with geological map 1:40.000.
Vescovi, E., Ravazzi, C., Arpenti, A., Finsinger, W., Pini, R., Valsecchi, V., Wick, L., Ammann, B., Tinner, W., 2007. Interactions between climate and vegetation on the southern side of the Alps and adjacent areas during the Late-glacial period as recorded by lake and mire sediment archives. Quat. Sci. Rev. 26, 1650–1669.
Walker, M.J.C., Björck, S., Lowe, J.J., Cwynar, L.C., Johnsen, S.J., Knudsen, K.L., Wohlfarth, B., INTIMATE Group, 1999. Isotopic events in the GRIP core: a stratotype for the Late Pleistocene. Quat. Sci. Rev. 18, 1143–1150.
Wiles, G.C., Calkin, P.E., 1994. Late Holocene, high-resolution glacial chronologies and climate, Kenai Mountains, Alaska. Geol. Soc. Am. Bull. 106, 281–303.